



# Soil moisture products consistency for operational drought monitoring in Europe

Jaime Gaona<sup>1</sup>, Davide Bavera<sup>2</sup>, Guido Fioravanti<sup>3</sup>, Sebastian Hahn<sup>4</sup>, Pietro Stradiotti<sup>4</sup>, Paolo Filippucci<sup>1</sup>, Stefania Camici<sup>1</sup>, Luca Ciabatta<sup>1</sup>, Hamidreza Mosaffa<sup>1</sup>, Silvia Puca<sup>5</sup>, Nicoletta Roberto<sup>5</sup>, Luca Brocca<sup>1</sup>

5 <sup>1</sup>Research Institute for Geo-Hydrological Protection, National Research Council, Perugia, 06126, Italy.

<sup>2</sup> Arcadia SIT, Milano, 27029, Italy.

<sup>3</sup> Joint Research Center, Ispra, 21027, Italy.

<sup>4</sup> Technische Universität Wien, Department of Geodesy and Geoinformation, Vienna, 1040, Austria.

10 <sup>5</sup> Italian Civil Protection, Rome, 00193, Italy.

*Correspondence to:* Jaime Gaona (jaimegaonagarcia@cnr.it)

## Abstract

15 The roadmap to enable operational soil moisture (SM) monitoring for meteorologic and hydrological early warning is challenged by the uncertainty within the available remote sensing and modelling products. This study addressed two relevant uncertainties: the residual trends in the series and the spatial consistency. While the latter has been often revisited to validate remote sensing and modelling products against in-situ data, the former is often disregarded in studies addressing SM changes.

20 This study evaluated three SM products: (1) the Satellite Application Facility on Support to Operational Hydrology and Water Management (H SAF) active Advanced SCATterometer (ASCAT)-derived dataset, (2) the passive subset of the European Space Agency (ESA) - Climate Change Initiative (CCI<sub>p</sub>), and (3) the modelled dataset from the European Drought Observatory (EDO). The analysis was carried out over Europe in the period 2007-2022 at 10-day temporal scales.

25 We obtained that even these popular datasets are subject to patches of spatial inconsistency and residual trends when compared to the in-situ data from the International Soil Moisture Network (ISMN). In view of the great complementarity shown by the active and passive remote sensing and the modelled SM estimates, two merged products are proposed and tested against in-situ data. Results indicate that combining H SAF ASCAT, CCI<sub>p</sub> and EDO equals or surpasses the spatial and temporal consistency of the individual SM products alone, even when only the near-real-time products of H SAF ASCAT and EDO are combined. Thus, merging remote sensing and modelled SM products is advantageous for enhanced spatial and temporal  
30 operational monitoring of SM at European scale.

## Keywords

Drought, Soil moisture, Remote sensing, Model Spatial validity, Residual trends



## 1 Introduction

35 Soil moisture (SM) is a key state variable of the water cycle, fundamental in the study of climate change impacts. SM anomalies  
are among the first warnings of altered conditions not only in the hydrological domain (Ford et al., 2015; Brocca et al., 2016;  
Li et al., 2023) but also, in many critical zone processes (Seneviratne et al., 2010; Green et al., 2019; Bolten and Crow, 2012).  
Aiming to track such challenging pace of alteration, the need to characterize SM change was encouraged long ago (Owe et al.,  
1999). Given the heterogeneous nature of a variable determined by soil and land use variability (Wilson et al., 2004; Zucco et  
40 al., 2014), and the persisting lack of funding to expanding or even maintain SM observation networks (Dorigo et al., 2021),  
alternatives were necessary to enable the systematic monitoring of SM. The emergence of remote sensing (RS) sensors and  
missions (Schmugge, 1983; Wigneron et al., 2000, Entekhabi et al., 2010) and the fast development of SM-capable modelling  
tools (e.g. Sheffield and Wood, 2007; Dirmeyer et al., 2006; De Roo et al., 2000) enabled widespread use of SM data for earth  
systems analysis (Ochsner et al., 2013).

45 Two approaches have primarily dominated SM RS technologies from their inception: active and passive microwave  
instruments to detect naturally emitted microwave radiation (radiometer) or the reflection of the emitted electromagnetic  
radiation (radar) (Schmugge, 1983). Early satellite missions carrying active sensors were not primarily designed nor deployed  
on-board dedicated soil moisture satellites, but they were found useful for the identification of SM beyond their initial  
50 meteorological operation (Loew et al., 2013). Such pioneering satellite missions with active sensors include the series of  
European Remote Sensing Satellites (ERS-1/-2) and the series of Meteorological Operational Platforms (Metop-A/-B/-C). The  
Satellite Application Facility on Support to Operational Hydrology and Water Management (H SAF) provides surface SM  
(SSM) estimates derived from ASCAT on-board the series of Metop satellites since 2008 with near-real-time operability  
(Albergel et al., 2012).

55 The passive group of sensors include the pivotal Advanced Microwave Scanning Radiometer-Earth Observing System  
(AMSR) mission onboard the Aqua satellite launched in 2002 (Njoku et al., 2003) and the SM-dedicated European Space  
Agency (ESA) Soil Moisture and Ocean Salinity (SMOS) mission of 2009 (Wigneron et al., 2000). Their decisive  
contributions stimulated the systematic use of L-band passive data, whose retrievals of coarse resolution are less prone to  
60 interferences among the different microwave bands (Kim et al., 2013). However, the advantage of complementarity in between  
active and passive sensors was the reason for the Soil Moisture Active Passive (SMAP) mission initiative of NASA (Entekhabi  
et al., 2010). Unfortunately, the failure of the SMAP radar soon after launch left the ambition to join the virtues of active and  
passive SM retrievals to the merging methods of initiatives like the ESA Climate Change Initiative (CCI) Soil Moisture Version  
08.1 (Gruber et al., 2019), whose passive subset is used here (i.e. CCIp).

65



The complementary features of the active and passive RS SM datasets soon became object of interest (Scipal et al., 2008). Partly due to the possibility to compensate the SM retrieval difficulties of one technique with the advantages of the other, multiple studies explored the combination of either data of different RS types or of RS with modelled data. Most cases applying first the scaling of the cumulative distribution function (Reichle and Koster, 2004). Since then, different merging methods

70 have been proposed, from simple equal weighting of the products to least-square framework that assigns weights based on the error variances in between products (Yilmaz et al., 2012). To a great extent these developments lead to the release of combined passive and active global SM datasets (Liu et al., 2012), such as CCI. Combined products reportedly outperform single source products for SM evaluation (Dorigo et al., 2015; Wang et al., 2021).

75 In parallel to the development of RS SM datasets, a lot of progress has been done in modelled SM products, and a wide range of them is increasingly used and evaluated (Beck et al., 2021). From the case of land surface models to the one of the numerical models like LISFLOOD (LF) (De Roo et al., 2000), modelling schemes have been widely incorporated to meteorological forecasting, reanalysis and monitoring protocols (Van der Knijff et al., 2010). In particular, LF was adopted by as the primary tool for providing near real-time flood risk assessment at continental scale for European Flood Awareness System (EFAS) and

80 then used in the European Drought Observatory (EDO) for drought monitoring (Cammalleri et al., 2015). The flexibility of models is beneficial to evaluate SM sensitivity to the many factors of the complex soil system even under scenarios (Vereecken et al., 2016), but the high demand on data, intricate parametrization and the assumptions behind the structure of models may degrade the reliability of their estimates (Fatichi et al., 2016; Samaniego et al., 2013).

85 The RS, model-based as well as the merged SM products undergo validation using a variety of protocols, including the check for validity against in-situ data of the SM observation networks available in the area (Al-Yari et al., 2019) gathered by the International Soil Moisture Network (ISMN) (Dorigo et al., 2011; Dorigo et al., 2021) are crucial for this purpose. However, besides the validity tests that usually evidence limitations of coverage, continuity and scale (Loew et al, 2013; Peng et al., 2017), there is a recurrent aspect of validation that requires major attention: the identification of spurious tendencies (Gruber

90 et al., 2020; Wagner et al, 2022) affecting the interpretation of the spatiotemporal features of SM data in the context of climate change. Beyond prominent works that proved fundamental reporting change in SM series (e.g. Dorigo et al., 2012; Albergel et al., 2013a; Feng and Zhang, 2015; Cammalleri and Vogt, 2016), multiple studies, even when proposing effective approaches to identify trends, may have reported tendencies that may be artifacts of the SM series. Explicit analyses of the uncertainties within SM datasets have always represented a minority among the studies using SM data, either from the time pioneering SM products appeared (e.g. Künzer et al., 2008; Draper et al., 2009; Liu et al., 2012) or at our time when multiple SM products release frequent new version with improved processing methods (Karthikeyan et al., 2017) or new products using different approaches are incorporated (Zwieback et al., 2017). Key studies on this topic reported temporal instabilities of the series (e.g. artificial trends Dorigo et al., 2010; temporal instability Albergel et al., 2013b; or inherited parametrization uncertainties, Crosson et al., 2005). Specific audit of the uncertainties of the data is thus required (Peng et al., 2021a; Brocca et al., 2017b).



100

Consequently, at least these matters require thorough revision before proposing a systematic application of SM products for trend identification and operational monitoring. Aiming to contribute to the proper use of SM products in consonance to their strengths and limitations, this article evaluates three SM products of passive RS, active RS and model-based nature and of near-real time capabilities to better explore their individual and combined potential for the operational monitoring of SM. The following activities are targeted:

105

- Assessing the correlation of ESA CCIp, H SAF remote sensing ASCAT-SSM-CDR-12.5km, including both Version 7 (H120) and Version 8 (H121), with the model-based EDO SM data.
- Discussing the suitability of product merging of active and passive RS SM with model-based SM for operational monitoring, focusing on near-real time product capabilities.
- Evaluating the performance of the active and passive RS SM, model-based SM and merged SM products against in-situ observation of the ISMN in Europe.
- Describing the trends of these diverse SM datasets and their combination and discussing their specific performance and its impact on trend detection.

110

## 2 Study area

115 The study focuses on Europe with additional coverage of the areas surrounding the Mediterranean basin. EDO includes data produced by a defined setup of the hydrological model LF whose domain covers almost the whole European continent and the Mediterranean region, approximately in between latitudes 25 to 75°N and longitudes 25°W to 50°E. Most RS products are of global scope, and therefore suitable for multiple-scale analysis from the global scale to the scale of their spatial resolution. However, some RS SM products are somehow limited at high latitudes (latitudes higher than 60°N) due to physical (frozen soil, snow cover) or technical limitations of their sensors (angle of view). The area of study is displayed using Lambert Azimuthal Equal Area (EPSG: 3035) centred at 50°N, 15°E. (Fig. 1).

120

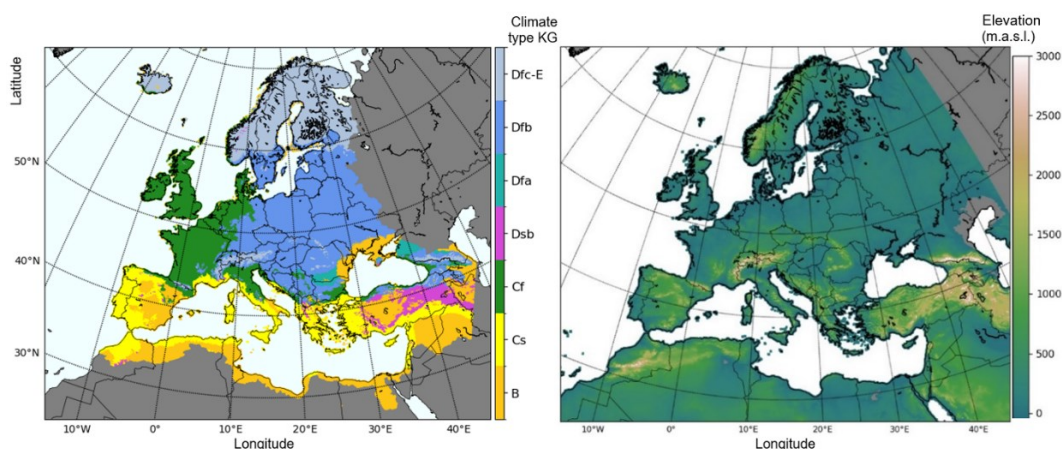




**Figure 1: a) Climatic classification based on Köppen-Geiger climate types of Europe and the circum-Mediterranean region (Beck et al., 2018). Not coloured areas represent climate types excluded from analysis. b) Elevation map based on ETOPO\_2022 by NGDC**  
125 **NOAA.**

The scope at the European scale grants the existence of multiple climatic regions of particular environmental characteristics (Fig. 1b) within the study area. Not only in terms of latitude, from the tundra of northern Scandinavia to the semiarid regions of the Mediterranean basin, but also from sea level to alpine altitudes, Europe offers a wide range of climates (Fig. 1a: Map of climatic areas based on the classification of climates of Köppen-Geiger (Beck et al., 2018). At least three out of five of the main climatic domains of this classification can be found across the continent, the type B climate of semi-arid to arid regions defined by precipitation, and two temperate climates determined by the annual temperature range: the type C of low annual temperature range modulated by sea influence and the type D of wide annual temperature range prevalent in the continental inlands. Other geographical aspects beyond climatic zoning such as land cover have not been considered but play a role in uncertainties of the RS SM data retrieval such as biomass content or dense vegetation (Pfeil et al., 2018; Ma et al., 2019; Ikonen et al., 2018) and are only secondary object of comments in discussion. (Fig. 2: Map of ISMN networks with land cover)

130  
135

### 3 Materials and methods

#### 3.1 Remote sensing soil moisture data

##### 3.1.1 Active microwave soil moisture

##### 140 *H SAF soil moisture products*

The C-Band real aperture radar system of ASCAT onboard Metop-A satellites since 2006, Metop-B since 2012 and Metop-C since 2018, collect active microwave data at sun-synchronous near-polar orbits that is processed using the TU Wien SM retrieval algorithm to generate the H SAF SSM products. The products used here ASCAT-SSM-ICDR-12.5km-v7 (H120) (<https://hsaf.meteoam.it/Products/Detail?prod=H120>) and the upcoming ASCAT-SSM-CDR-12.5km-v8 (H121) cover the study period 2007-2022 and incorporate the last improvements on signal processing and correction (Hahn et al., 2017). This remarkable length, continuity and coverage of the ASCAT-derived H SAF SSM products have popularized RS SSM for multiple applications (Brocca et al., 2017). The H SAF products H120 and H121 used here have a spatial sampling of 12.5 km arranged on a Fibonacci spiral grid at a spatial resolution of 25 x 25 km. SSM is expressed as degree of saturation (0% dry soil, 100% fully saturated soil) of the first few centimeters of the soil (< 5 cm) as water volume present in the soil relative to pore volume (Wagner et al., 1999; Naeimi et al., 2009).

145  
150

##### 3.1.2 Passive microwave SM based on C-band and L-Band retrievals:

##### *ESA CCI passive soil moisture dataset*



155 ESA CCI passive dataset (CCI<sub>p</sub>) is the subset of ESA CCI SM v08.1 (Dorigo et al., 2017; Gruber et al., 2019) (https://climate.esa.int/en/projects/soil-moisture/) based on merging of passive sensors only. The data is provided globally at a sampling of 0.25° x 0.25° with more frequent spatial gaps in the early years of the dataset (Loew et al., 2013). Alpine or boreal regions and densely forested areas show spatial and temporal gaps of the retrievals due to frozen soils or the canopy cover attenuation (Dorigo et al., 2017). The daily temporal resolution is available from November 1978 to the end of 2023. The merging is conducted on the basis of the signal-to-noise ratio and scaled against SM dynamic ranges of GLDAS-Noah v2.1 land surface model (Rodell et al., 2004) and break-adjusted (Preimersberger, 2020).

## 160 **3.2 Model-based soil moisture data**

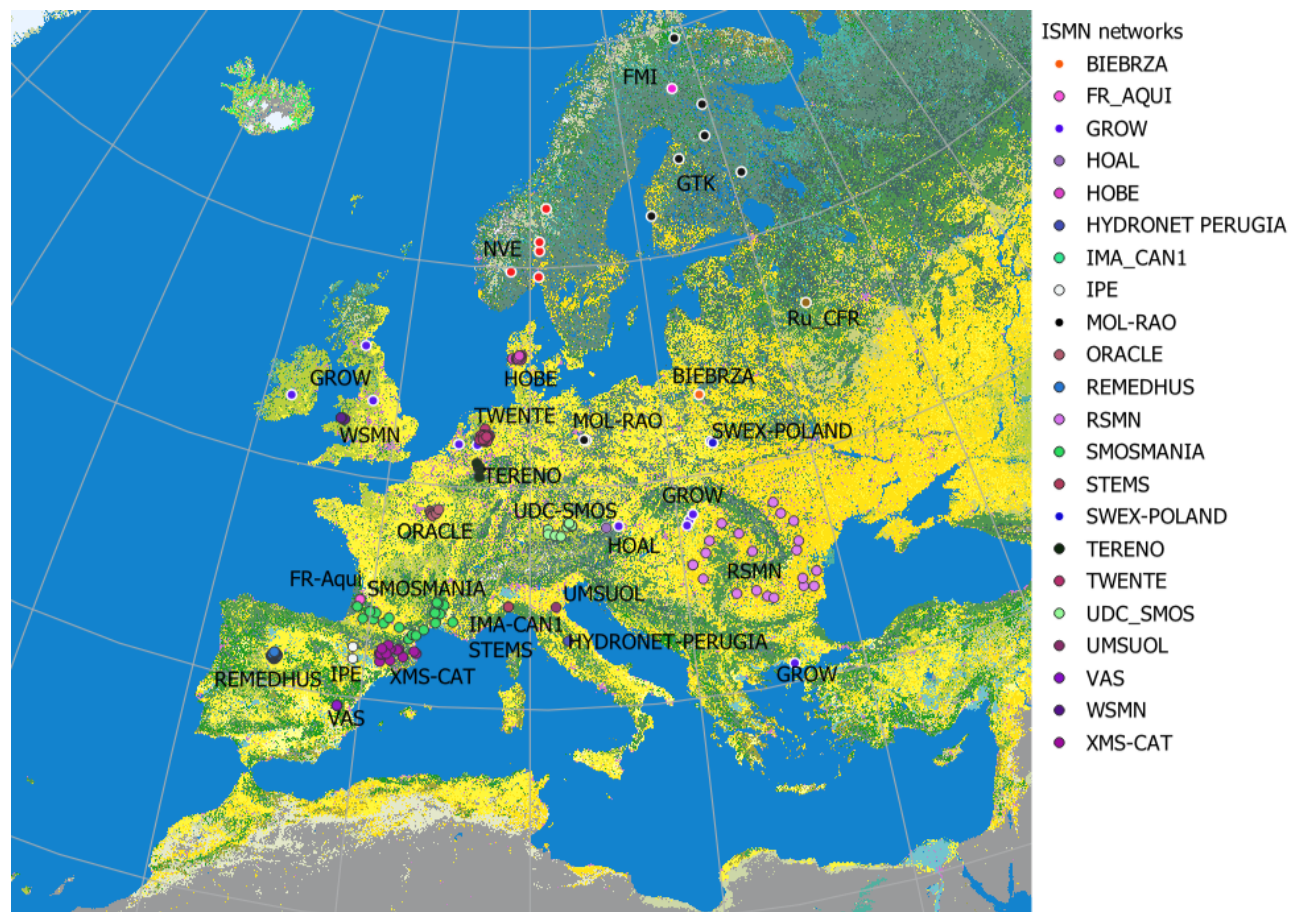
### **3.2.1 The European Drought Observatory (EDO)**

165 EDO (https://edo.jrc.ec.europa.eu) provides LISFLOOD (LF) model-based SM estimates. LF is the distributed rainfall-runoff model initially developed for flood forecasting by the Land Management and Natural Hazards Unit of the Joint Research Centre (JRC) of the European Commission. The first two layers (corresponding to the root depth) of the three layers provided by the model when simulating the water balance of the catchment are considered for the commutation of the SM index. The dataset has a 5 × 5 km grid cell size. To perform all the analyses, H120 / H121 and CCI<sub>p</sub> SM products are regridded to this finer spatial resolution of EDO. The dataset spans from 1991 to present at daily temporal resolution but is commonly provided at the 10-day period corresponding to the 1st, 2nd and 3rd third of the month.

## **3.3 In-situ soil moisture data**

### 170 **3.3.1 The International Soil Moisture Network (ISMN)**

The International Soil Moisture Network (ISMN, https://ismn.geo.tuwien.ac.at/, Dorigo et al., 2021) is the collective initiative supported by ESA to compile the data of multiple networks observing SM around the globe originated for various purposes. Since the SM data became essential for RS, the ISMN aims to favor the harmonization of the SM observations. As of May 2024, the ISMN database hosts 80 networks data all over the world, comprising the 26 networks across Europe included in this study with data available in the study period 2007-2022 (Table S1, supplementary material). The networks comprise a diverse but uneven range of climates and land cover (Table S1, supplementary material). The assorted scales and measuring settings of the included ISMNs are of challenging spatial representativity compared to the distributed RS data (Gruber et al., 2013).



180 **Figure 2: (a) Location of the SM networks of the ISMN initiative in Europe superimposed over ESA CCI Land Cover 300m 2015 (Kandice et al., 2023). Yellow/green colours represent crops/natural vegetation.**

### 3.4 Methodology

#### 3.4.1 Preprocessing

Initial datasets feature diverse spatial and temporal scales. For this reason, both spatial and temporal pre-processing of the  
185 datasets is required. In spatial terms, the datasets are re-gridded to the reference spatial grid of EDO of 5 x 5 km using the  
search of nearest neighbours of KD-Tree algorithms. In the case of H120 and H121, a transformation from the original  
Fibonacci swath geometry used by ASCAT to the regular grid geometry of the other datasets is required. The temporal time  
step defined for the analyses is the 10-day time scale, which is the time scale followed by the EDO. Each of the three reference  
190 dates per month arranged in this tri-monthly basis represent the average conditions of a third of the month (i.e. from the 1<sup>st</sup> to  
the 10<sup>th</sup>, from the 11<sup>th</sup> to the 20<sup>th</sup>, and from the 21<sup>th</sup> to the 31<sup>th</sup> of a month). The daily values of the initial datasets in between  
these two of these three reference dates are aggregated to the first of the reference dates. In the case of H121, the aggregation



to the 10-day time scale is computed by directly aggregating the hourly-scale datasets within the 10-day period during the computation of the Soil Water Index (SWI) from the original SSM given in degree of saturation. The computation is based on the exponential smoothing filter (Wagner et al., 1999b; Albergel et al. 2008) that converts the surface saturation degree,  $ms(t)$ , into the  $SWI(t)$  (Eq. (1)):

$$SWI(t) = \frac{\sum_i^n m_s(t_i) e^{-\frac{t-t_i}{T}}}{\sum_i^n e^{-\frac{t-t_i}{T}}} \quad (1)$$

where, regardless of the units of product, the soil moisture retrieval at time  $t_i$  is  $SM_{sat}$ , the time lag introduced with the filter is  $T$ , and  $t$  represents the 10-day time step.  $T$  was set to 10 days for all the products. The SWI ranges between 0 and 1 from dry to wet conditions. More than 3 retrievals in the 10-day interval  $t$  were prescribed for calculating SWI, following Pellarin et al., (2006). Due to the exponential filter smoothing effect (and delay) of  $ms(t)$  the range of  $SWI(t)$  varies in a narrower range than the  $[0,1]$  degree of saturation range.

The 10-day time scale is used for the intercomparison and evaluation of the products against the ISMN while the monthly scale is adopted for the trend analysis of SM anomalies. The SM anomalies are computed by removing the seasonal cycle, which is defined by the mean SM value of each month of the year. These twelve mean SM values are obtained by averaging all 10-days SM within each calendar month occurring along the study period. The SM anomaly is then calculated as the ratio of deviation of SM of any month from the mean SM of that month.

### 3.4.2 Performance metrics

The Pearson's correlation coefficient (R) is used to quantify the correspondence between H120 and H121, CCIp and EDO SM products and the ISMN SM data. The triple collocation analysis (TCA) (Stoffelen, 1998; Scipal et al., 2008) is also used to estimate the random error variances of the collocated H120 / H121, CCIp, and EDO triplets. The error model of TCA is applied assuming linearity of SM retrievals, stationarity of signal and independence of errors from signal or in between product errors (Gruber et al., 2016; Massari et al., 2017; Filippucci et al., 2021) (Eq. (2)):

$$X = \alpha_X + \beta_X \theta + \varepsilon_X \quad (2)$$

where the spatially and temporally collocated datasets are compiled in the dataset  $X \in [H120 \text{ or } H121, CCIp, EDO]$ , the soil moisture is  $\theta$ , and  $\alpha_X$  is the systematic additive error behind the offset between the temporal and the true mean of  $\theta$ . The  $\beta_X$  is the coefficient of multiplicative biases of  $X$ , and noise is represented by  $\varepsilon_X$ . Even in the case of SM whose random error can depart from a gaussian distribution, the error variance can be expressed as in McColl et al. (2014) (Eq. (3)):

$$\sigma_\varepsilon = \left[ \begin{array}{c} \sqrt{Q_{11} - Q_{12}Q_{13}/Q_{23}} \\ \sqrt{Q_{22} - Q_{12}Q_{23}/Q_{13}} \\ \sqrt{Q_{33} - Q_{12}Q_{23}/Q_{12}} \end{array} \right] \quad (3)$$



220 where  $Q_{ij}$  is the covariance of dataset  $i$  against  $j$ , which leads to the expression of TCA correlation scores  $R\_TCA$  (Eq. (4)), which is a relative measure against the unknown truth:

$$R\_TCA = \frac{\sqrt{Q_{12}Q_{13}/Q_{11}Q_{23}}}{\sqrt{Q_{12}Q_{23}/Q_{22}Q_{13}}} \quad (4)$$

The TCA approach is also suitable for merging RS SM products (Gruber et al., 2017). TCA scores are computed for each product and across different climates (Beck et al., 2018).

### 225 3.4.3 Definition of the products merging RS and model-based SM data

Merging is obtained by combining the SM estimates of the intervening products proportionally to weights based on their different  $R\_TCA$  scores of the TCA. The triplets of TCA generating the  $R\_TCA$  scores are equalized in dynamic range matching their cumulative distribution functions (CDF) (Brocca et al., 2010b). The expression to merge the SM product is:

$$SM_{merg2} = \omega_{H\ SA F} \cdot R\_TCA_{H\ SA F} + \omega_{CCI p} \cdot SM_{CCI p}^* + \omega_{EDO} \cdot SM_{EDO}^* \quad (5)$$

230 where  $\omega_i$  is the relative weight of each product's  $R\_TCA$  scores, obtained from Eq. (6):

$$\left\{ \begin{array}{l} \omega_{H\ SA F} = \frac{R\_TCA_{H\ SA F}}{R\_TCA_{H\ SA F} + R\_TCA_{CCI p}^* + R\_TCA_{EDO}^*} \\ \omega_{CCI p} = \frac{R\_TCA_{CCI p}^*}{R\_TCA_{H\ SA F} + R\_TCA_{CCI p}^* + R\_TCA_{EDO}^*} \\ \omega_{EDO} = \frac{R\_TCA_{EDO}^*}{R\_TCA_{H\ SA F} + R\_TCA_{CCI p}^* + R\_TCA_{EDO}^*} \end{array} \right. \quad (6)$$

Where  $R\_TCA_{H\ SA F}$ ,  $R\_TCA_{CCI p}^*$  and  $R\_TCA_{EDO}^*$  are the TCA correlation scores of H SAF (H120 or H121), CCIp and EDO. CDF matching (\*) is applied in reference to the product without the mark (H SAF H120 or H121) to equalize the dynamic ranges. The two products obtained with this procedure of merging H SAF (H120 or H121), CCIp and EDO or only H SAF (H120 or H121) and EDO are hereafter respectively denominated 'MERG\_h121\_3', and 'MERG\_h121\_2'.

### 3.4.4 Evaluation against in situ data

The evaluation of SM products against in-situ data used all available ISMN within Europe for the period 2007-2022 despite the existing several factors of uncertainty regarding the quality of the data (e.g. representativity or SM range). The ISMN stations whose data availability is shorter than that of the study period were paired to the corresponding equal period of the RS H120/H121, CCIp, the model-based data from EDO or their combination. All products were also aggregated to the reference 10-days scale of EDO. Pearson correlations to evaluate RS and model-based against the ISMN records were computed by extracting the corresponding time series of RS and modelled datasets at the locations of the stations of the ISMN networks, defined by their latitude and longitude, using KD-Tree algorithms of nearest neighbours.



### 3.4.5 Trend analysis

245 In this work, the Mann-Kendall (MK) (Mann, 1945; Kendall, 1948) methodology was considered to evaluate SM anomaly trends by the significance of the monotonic upward or downward trends. The lack of trend is indicated with a valid null hypothesis when data is independent and randomly distributed. The  $Z$  statistic rejects or accepts the existence of trend, based on the statistic  $S$ :

$$S = \sum_{i=1}^{n-1} \sum_{j=i+1}^n \text{sgn}(X_j - X_i) \quad (7)$$

$$250 \quad \text{Sgn}(X_j - X_i) = \begin{cases} 1 & \text{if } (X_j - X_i) > 0 \\ 0 & \text{if } (X_j - X_i) = 0 \\ -1 & \text{if } (X_j - X_i) < 0 \end{cases} \quad (8)$$

$$Z = \begin{cases} \frac{S-1}{\sigma} & \text{if } S > 0 \\ 0 & \text{if } S = 0 \\ \frac{S+1}{\sigma} & \text{if } S < 0 \end{cases} \quad (9)$$

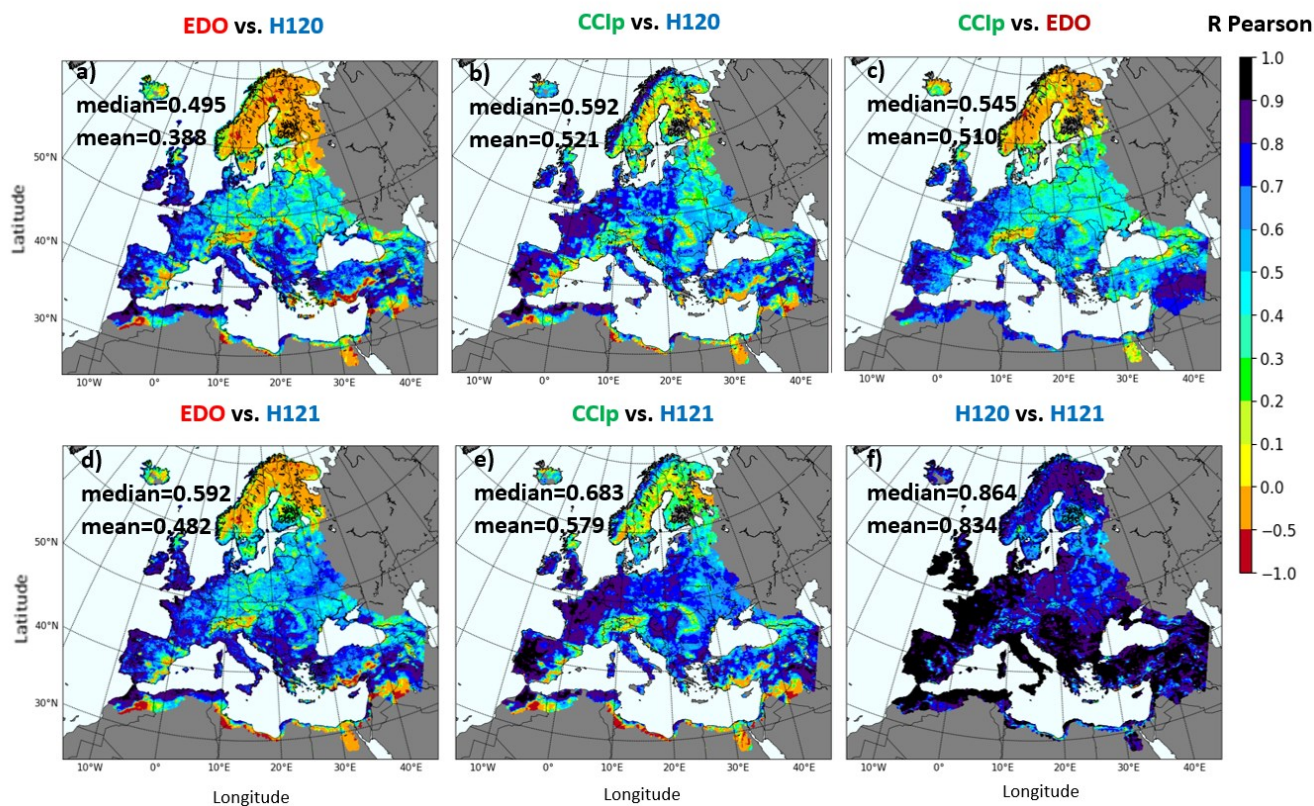
where  $X_j$  and  $X_i$  refer to the comparison of each value of the series of length  $n$  to the rest of values, so that the sign function (Eq. (8)) adds or subtracts from the rank expressed by  $S$  and tested with  $Z$ . We consider a significance level of 0.05, corresponding to values of  $Z > 1.96$ , to reject the null hypothesis and consider that the trend is significant (Rahmani et al., 255 2015).

## 4 Results and discussion

### 4.1 Characterizing the spatiotemporal concurrence between SM products

#### 4.1.1 Linear correlation analysis

The temporal correlation quantifies the correspondence between EDO, CCIp and H120 or H121. The correlation between 260 CCIp (Fig. 3b-e) gets the highest values either using H120 ( $R_{\text{median/mean}}=0.59/0.48$ ) or H121 (0.68/0.58). H121 version induces a notable improvement of the scores in respect to H120 also for the correlation with EDO (Fig. 3a-d) (from  $R=0.50/0.39$  using H120 to  $R=0.59/0.48$  using H121). The EDO-CCIp correlation remains intermediate compared to the others ( $R=0.55/0.51$ ) (Fig. 3c). Results indicate differences between the products over some areas of the continent. Products agree with  $R > 0.7$  over the British Isles except for Scotland, Benelux, western areas of Germany, France except the Alps, the Atlantic 265 basins of Iberia and some Mediterranean areas (e.g.: Peng et al., 2021b; Parinussa et al., 2014; Brocca et al., 2011). Multiple other regions in the Mediterranean basin display  $R > 0.5$  in line with previous reports (e.g.: Juglea et al., 2010; Brocca et al., 2010b; Duygu et al., 2019). Only continental central and NE Europe show less consensus ( $R < 0.4$ ) between products, particularly when EDO intervenes.



270 **Figure 3:** Map of spatial R-Pearson correlation in between a) EDO and H120, b) CCIP and H120, c) CCIP and EDO, d) EDO and H121, e) CCIP and H121, f) H120 and H121.

The mismatch between RS and EDO SM data in eastern Europe may be partly attributable to the uncertainty of LF model during winter (Cammalleri et al., 2015), especially since RS SM data is increasingly reliable in boreal areas (Ikonen et al., 2018). The water fraction may also interfere over lake areas of NE Europe (Paulik et al., 2014), but snow cover has been long  
 275 considered the prevalent cause of blurred determination of SM in *D-E* type climates, including mountains, with higher impact over EDO than over RS data (Laguardia and Niemeyer, 2008).

However, the apparent SW-NE gradient of consistency in between SM products attributed to snow prevalence may be SM regime-related, as it corresponds to the gradient of SM regimes depending on water or energy-dominated conditions (Denissen  
 280 et al., 2020, Fig. S1). The areas most influenced by westerlies (*C* climate types) of contrasted winter-summer SM regimes are the ones where SM products concur the most. Conversely, *D* climate types of East Europe that tend to sustain water-dominated SM regimes during summer exhibit the lowest similarity. Such SM-regime implications may require further analysis but have been recognized as impactful at least on the backscattering of active RS SM products (Wagner et al., 2022).



285 Topography (Fig. 1b) is also an important factor inducing uncertainty in the SM products in rough areas of Iberia (Escorihuela and Quintana-Seguí, 2016), north Africa, south Greece and Anatolia where SM retrievals are also prone to subsurface scattering of either C-band (ASCAT) or L/Ku-band active sensors (McColl et al., 2013; Wagner et al., 2022).

#### 4.1.2 Triple collocation analysis

TCA provides an accurate quantification of the correspondence in between SM products and in respect to the unknown reality (Stoffelen et al., 1998; Gruber et al., 2016). TCA results differ from the linear correlation analysis (Fig. 4 vs. Fig. 3). In the triplet of H120, CCIp and EDO, H120 scored in between EDO and CCIp (Fig. 4a<sub>1</sub>-c<sub>1</sub>). However, H120 seems fairly accurate in line with reports against ERA5Land (Pierdicca et al., 2015a). Therefore, when the improved version H121 is used in the triplet, it leads the scores (Fig. 4a<sub>2</sub>-c<sub>2</sub>), including over *D* and *E* type climates (Fig. 5). CCIp leads the scores in the triplet adopting H120 (Fig. 4c<sub>1</sub>), which was already remarkable because only CCI combined was reported superior to H120 before (Al-Yaari et al., 2019; Fan et al., 2022). CCIp remains second in R\_TCA in the triplet including H121, but in this case even EDO may achieve equal or better scores among climate differences. Nonetheless, EDO displays the lowest R\_TCA scores in both triplets using H120 and H121, especially in the NE of Europe (Fig. 4a<sub>1</sub>-a<sub>2</sub>). Multiple studies reported difficulties of models on snowed/frozen areas (Naeimi et al., 2012), but low scores are shown by all products in high latitudes / elevations (climate type *Dfc-E*) (Fig. 5).

300

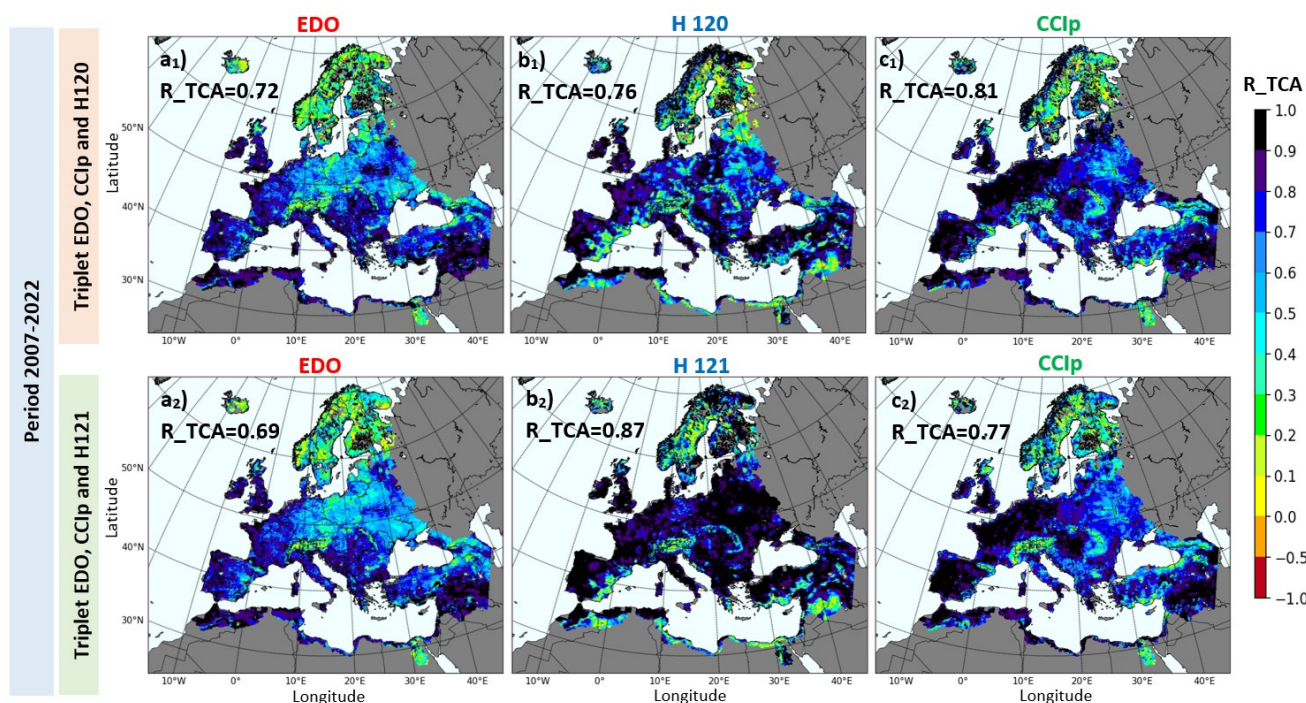
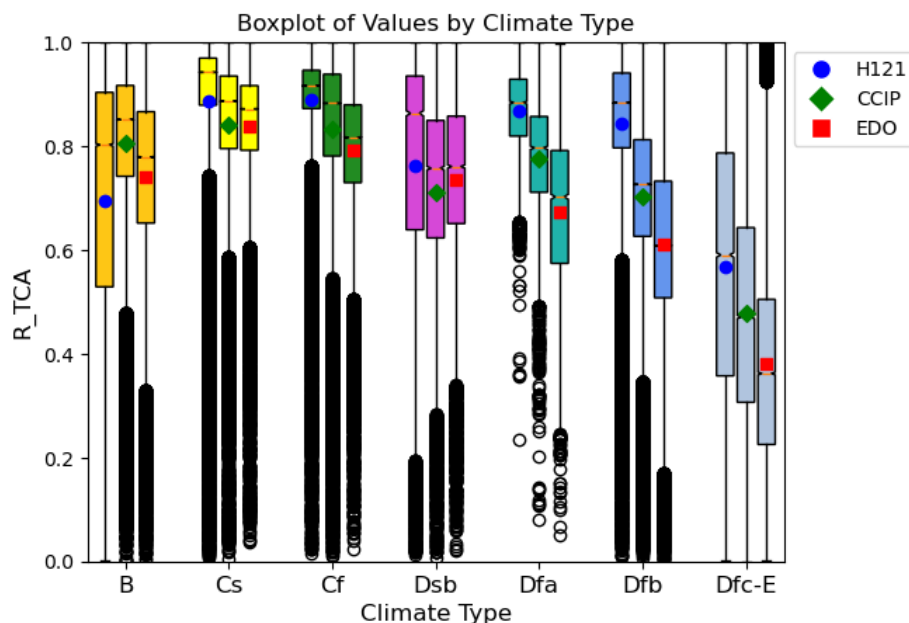


Figure 4: Maps of R\_TCA score of triple collocation analysis of the period 2007-2022 of the triplet of the (a<sub>1</sub>) modelled-based EDO, (b<sub>1</sub>) the active RS H120 and c<sub>1</sub>) the passive RS CCIp SM products. The second triplet (a<sub>2</sub>, b<sub>2</sub>, c<sub>2</sub>) just replicates the former with H121 in b<sub>2</sub>) replacing the version H120.



305 **Figure 5: Boxplots of triple collocation score ( $R_{TCA}$ ) of the model-based EDO (boxplots with red square indicating the mean) the active RS H121 (indicated with blue circles) and the passive RS CCIP SM product (depicted in green rhombus) in between different types of climates (colored as Fig.1b).**

The pattern of high consistency over western Europe (type *C* climate) (Fig. 5) has been already reported for EDO, H120 or CCI (LF, Cammalleri et al., 2017; ASCAT, Chen et al., 2018; CCI, ERA-5Land, Pierdicca et al., 2015b; CCI-ERA-Interim, 310 Deng et al., 2019). Sometimes attributed to coverage but also subject of discussion about the distinct modes of SM variability in Europe (seasonal in the west but of long-term nature in the east: Fig 11 of Piles et al., 2019). The prominent spots around urban areas due to urban backscattering visible in H120 are solved in H121. This underlines the relevance of updates incorporating processing improvements. However, the reduced signal in SE Spain that corresponds to the reported backscattering of arid areas (Wagner et al., 2022) or alternatively related to the autocorrelation error common in low LAI areas 315 (Dong and Crowd, 2017) remain. Similarly, swampy areas like the Pinsk/Pripet River floodplain in between Belarus and Ukraine that downgrade both H120/H121 and CCIP signals remain better covered by EDO. A bit to the west of this area, a diagonal of CCIP  $R_{TCA} \leq 0.8$  in between northeast Germany and Ukraine is prone to radio frequency interference (Oliva et al., 2016) as shown by the filtering of SMAP (Mohammed et al., 2016). Hence, even after updates, none of the products alone can fully characterize SM across Europe but can be overall complementary.

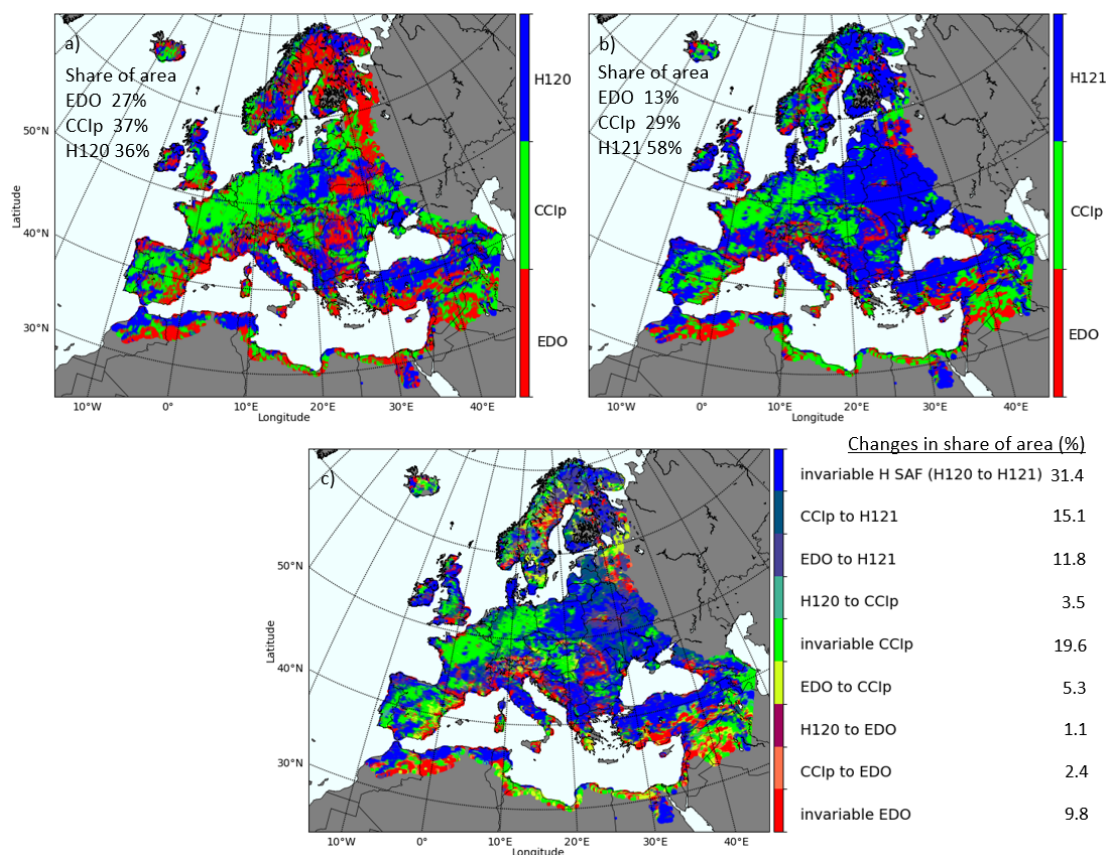
## 320 4.2 Characterizing the spatiotemporal concurrence between SM products

### 4.3.1 Linear correlation analysis

The convenience of merging RS and model-based SM datasets to get the full potential of their complementarity can be illustrated with the maps of best performing SM product over Europe (Fig. 6). Extensive areas of Europe are dominated by



CCIp, mostly in the areas facing west. Remarkably, these areas now better depicted by CCIp were H120-dominated areas in  
 325 the past (Leroux et al., 2013; Al-Yaari et al., 2014). The prevalence of CCIp is solid in those areas but slightly reduced in area  
 from H120 to the new version H121 (green areas, Figs 6a and 6b). The eastern part of the continent remains better portrayed  
 by H120 than CCIp, and even better by the H121. EDO that prevailed as best product in north latitudes is primarily replaced  
 there by H121, thus illustrating the notable progress of RS products despite their sensitivity to the challenging freeze-thaw  
 processes (Naeimi et al., 2012) or dense forest cover (Van der Molen et al., 2016; Ikonen et al., 2018). The prevalence of EDO  
 330 by the coast explained by the limited signal retrieval of RS sensors in the vicinity of the sea (Brocca et al., 2011; Kerr et al.,  
 2012; Portal et al., 2020) becomes also reduced with the new H121 version. Nonetheless, rough, arid or swampy areas of  
 uncertain RS data remain better recognized by EDO, followed by CCIp. In general, most changes when substituting H120 to  
 H121 in the triplets are favourable to H121, whose share of areas as best product increases from similar to CCIp to a dominating  
 58% (Fig. 6a vs. 6b). CCIp change to H121 contributed more than EDO change to H121 (Fig. 6c) to the dominance of H121  
 335 (Fig. 6b). EDO experiments more declined than CCIp in shared area.



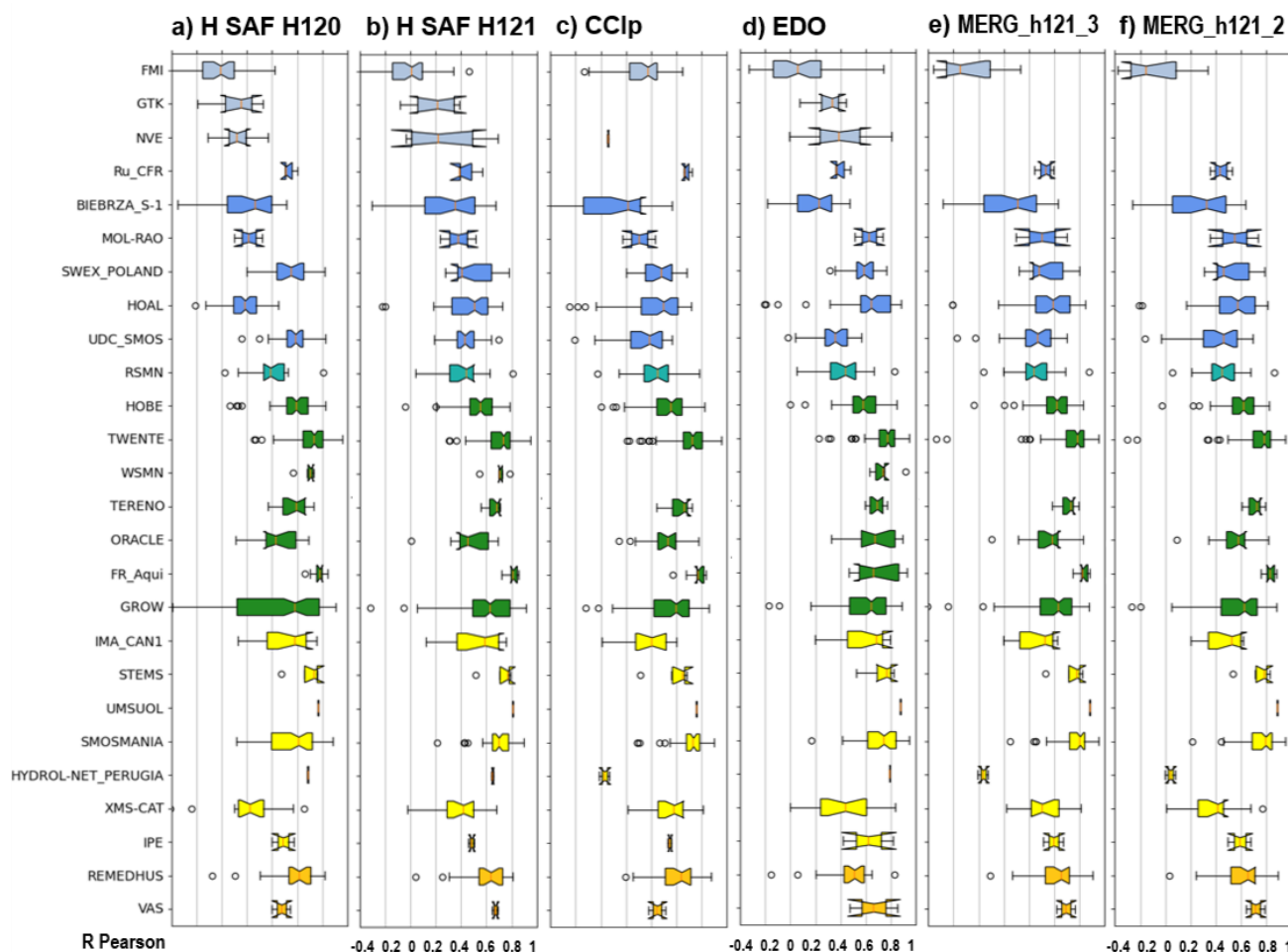
340 **Figure 6: Map of best performing SM product over Europe for a) the triplet H120, CCIp and EDO and b) the triplet H121, CCIp and EDO. c) Map identifying all changes of best product (from product x to product y) and the areas that stay invariably best estimated by each product with quantifications in % total area.**



The spatial prevalence of CCIP and H120 / H121 over western and eastern Europe respectively agrees with the climatic division in between *C* and *D* climates (Fig. 6b). Intrinsic hydroclimatic differences may be the cause, either as an expression of the distinct SM regimes as identified with self-organizing maps (Markonis et al., 2020; see Fig. 4), as expression of the oceanic vs. continental moisture (Gimeno et al., 2012) or due to distinct SM variabilities (Piles et al., 2019). Ecoregions, which also  
345 express hydroclimatic differences, have also evidenced differences in the consistency of SM estimates among products (Mazzariello et al., 2023). The depth of the active and passive RS SM retrievals might be also distinctly sensitive to the dominant rewetting process (Lun et al., 2021; Santos et al., 2022). Even though the reasons behind these differences are beyond our scope, they emphasize the complementarity of the active, passive and modelled SM products. Hence, it is reasonable to conceive operational products combining RS and modelled SM data (Parinussa et al., 2014; Peng et al., 2021b) with potential  
350 for SM monitoring. The two proposed merged products combine the best of the ASCAT derived products, H121, and EDO ('Merg\_h121\_2') or H121, EDO and CCIP ('Merg\_h121\_3'), and their performance is evaluated together with H121, CCIP, EDO against the ISMN data including trends.

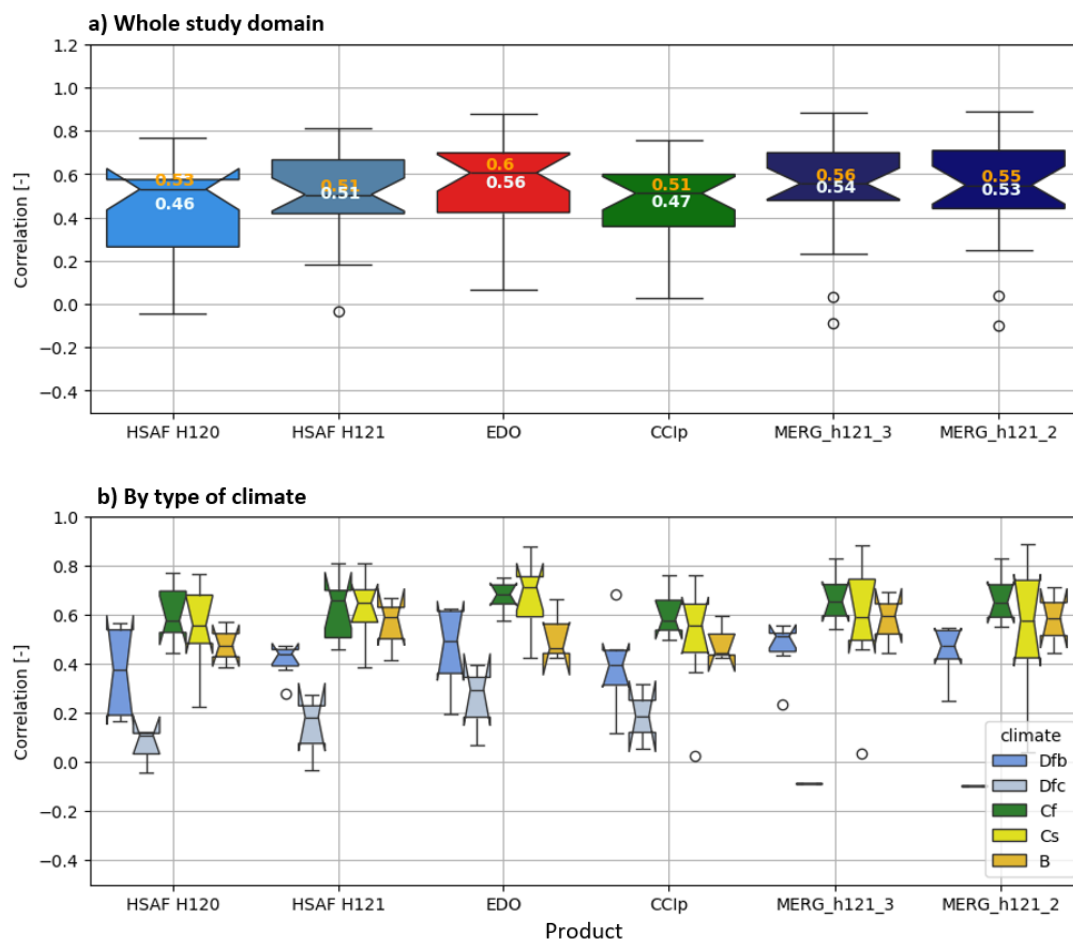
#### 4.3 Active, passive and model-based SM products against in-situ ISMN data

The consistency of RS, model-based and merged SM products considered in this study is compared to the data of the European  
355 networks of the ISMN for their coincident periods (Fig. 7). CCIP coherently agrees for most of the networks with its active counterpart, the H120 / H121 products, both in magnitude and spread of correlations despite being the product with the lowest overall R mean/median score at the ISMN ( $R_{CCIP}=0.47/0.51$ ). H120 / H121 active SM datasets perform second in terms of overall R Pearson correlation (Fig. 7) among the ISMN ( $R_{H120}=0.46/0.53$ ,  $R_{H121}=0.51/0.51$ ). H120 is the SM product showing the widest spread of correlations in some of the evaluated ISMN such as BIEBRZA\_S-1, GROW, GTK, XMS-CAT. The  
360 lowest correlation values are also seen in FMI, GTK, XMS-CAT networks. Apart from GROW network, prone to high uncertainty (Zappa et al., 2020), and XMS-CAT which length of series may be limited, FMI and GTK usually show poor correlation values with RS data (Kolassa et al., 2017; Ikonen et al., 2018) attributed to the dense boreal canopies challenging active and passive sensors (Petropoulos et al., 2015; Kerr et al., 2012).



365 **Figure 7: R Pearson coef. of a) H120, b) H121 c) CCip, d) EDO, e) the merged MERG\_h121\_3 (combining H121, CCip and EDO),**  
**and f) the merged MERG\_h121\_2 (combination of H121 and EDO) against in-situ SM data of the ISMN (names of networks in the**  
**leftmost column). The colour of the notched boxplots corresponds to Koppen Geiger climatic classes (gold colour=*B* climate class,**  
**yellow: *Cs*, Green: *Cf*, Blue: *Dfb*, Blue-green: *Dfa*, Ice blue: *Dfc-E*) assuming all stations of each network have same climate. In the**  
**Y axis ISMN networks sorted from the northernmost to the southernmost in latitude within each group of climate, and climates**  
**sorted from colder to warmer.**

Precisely over boreal areas of D-E climate types (Fig. 8b) are visible the clearest differences in R score across all products. The rather high R scores of EDO ( $R_{EDO}=0.56/0.6$ ) also show a downgrade in performance (Cammalleri et al., 2015) (Fig. 8) due to its better calibration for rain-dominated than for snow-dominated regimes (Salamon et al., 2019). The values of SM estimated by EDO agree to a great extent with those of H120 / H121 and CCip, which exceed globally, the mean/median scores of these RS products. The low performance of EDO over the UDC\_SMOS network may be related to challenging SM and floods in the upper Danube during the period 2007-2011 of UDC\_SMOS series (Wanders et al., 2014). EDO performs best at two local networks: UMSUOL and HYDRO-NET-PERUGIA.



380 **Figure 8:** a) Boxplots illustrating the distribution of the R Pearson correlation coef. of the active RS SM product H120 and H121, the passive CCip, the model-based EDO and the two suggested merged products with superimposed mean values in white and median values in yellow color. b) Boxplots of the products for the subsets of the different climate types. The notches represent the confidence interval of the median and when surpassing the interquartile ranges indicate uncertainty, partly due to a small size of the samples.

385 When the range of the notch surpasses the interquartile range of the boxplots in a network, which occurs in local-scale networks such as MOL-RAO, Ru\_CFR or VAS, RS might be unable to display the SM variability that local-scale networks can describe (Brocca et al., 2010a). EDO has the least prevalence of notched boxplots. Although the measuring technology plays a role because using less accurate techniques (e.g. GROW, BIEBRZA\_S-1, XMS-CAT) tend to show also more spread at the ISMN data (Dorigo et al., 2021), other factors such as land cover may be more influential. The higher spread (Fig. 7) or lower correlation (Fig. 8) of CCip over some networks of heterogeneous land cover or in the extremes of the range of soil moisture conditions of the ISMN networks (e.g. XMS-CAT or BIEBRZA, respectively), can be due to the coarser resolution of CCI  
 390 compared to H120 and H121 (Dorigo et al., 2010).



The results of the merged products in Fig. 7 and 8 indicate that the weighted combination of techniques surpass the performance of H120 / H121 versions and CCIp ( $R_{\text{MERG\_h121\_3}}=0.54/0.56$ ,  $R_{\text{MERG\_h121\_2}}=0.53/0.55$ ). Only EDO shows higher scores thanks  
395 to its higher performance over the areas of climate *Dfc-E* that are challenging for RS SM products (Fig. 7 networks in blue and ice-blue, and at sub-boxplots plots of types of climate at Fig. 8b). In the rest of climates *MERG\_h121\_3* and *MERG\_h121\_2* tend to reduce the spread of the scores at ISMN and slightly increase their value. Despite the lower tails of the merged products propagating from climate types such as *Cs*, *Dfc-E* with short, local or reduced number of series, their distribution of values is better than that of individual products, especially for the interquartile range (Q1-Q3 in dashed lines over the boxplots of Fig.  
400 8a). Climate types that prevail across the continent such as *B*, *Cf* and *Db* are the most benefited, except for EDO, by the merging. Here, the merged products adopt a rather balance weighting, but any other merging scheme favouring the best performing product in an area may notably enhance the performance of the merged products. Furthermore, the *MERG\_h121\_2* (combining H121 and EDO) almost equals the results of the *MERG\_h121\_3* product, which evidences that best performing products can be obtained even without using CCIp, emphasizing the possibility to obtain a merged product solely based on RS  
405 and modelling data available in near real-time.

#### 4.4 Evaluating the trends on SM databases and discussing the implications

Results of the analysis of trends of the monthly anomalies in the period 2007-2022 of H120 / H121, CCI and EDO exhibit spatial and temporal contrasts (Fig. 9). There is partial agreement between the RS products CCIp and H120 / H121 (Fig. 9a,  $c_1$  and  $c_2$ ) not only in wet anomalies but also in a few drying areas. The relatively higher agreement between CCIp and H121  
410 across the continent is due to the less extensive wet trend of H121 but is consistent with multiple validation studies in the area (Gruber et al., 2019; Preimesberger et al., 2020) and with reanalysis data (ERA5-Land, not shown here, Pierdicca et al., 2015a).

However, there is notable contrast between the drying trend of EDO (Cammalleri and Vogt, 2016) and the wet trend of H120 (Wagner et al., 2022) (Fig. 9b vs. b). While the products have a clearly prevailing trend (positive in EDO, negative in H120),  
415 they still agree in the sign of the trend in the areas of their non prevailing trend which indicated relative spatial agreement despite not agreeing on magnitude. Therefore, as EDO and H120 don't surpass CCIp range of trends, they can be considered as the products depicting the lower (EDO) and upper (H120) range of trend characterization. They both additionally agree in extensive significance of the trends which suggest inherent issues of the products with trends, and subsequently, the products with lesser extent of significant trends are considered here of better performance in line with works indicating trends might be  
420 less widespread than expected (Almendrea et al, 2022). The divergence between H120 and EDO and the different range of the significant trends between CCIp and EDO (Fig. 9) illustrate the need to refine products, which recent versions (e.g. H121) seem to have accomplished.

The merged products show intermediate characteristics as results of combining H121 and EDO (*MERG\_h11\_2*) or also CCIp  
425 (*MERG\_h121\_3*). Their trends become more balanced in sign and of lower magnitude compared to their original products.

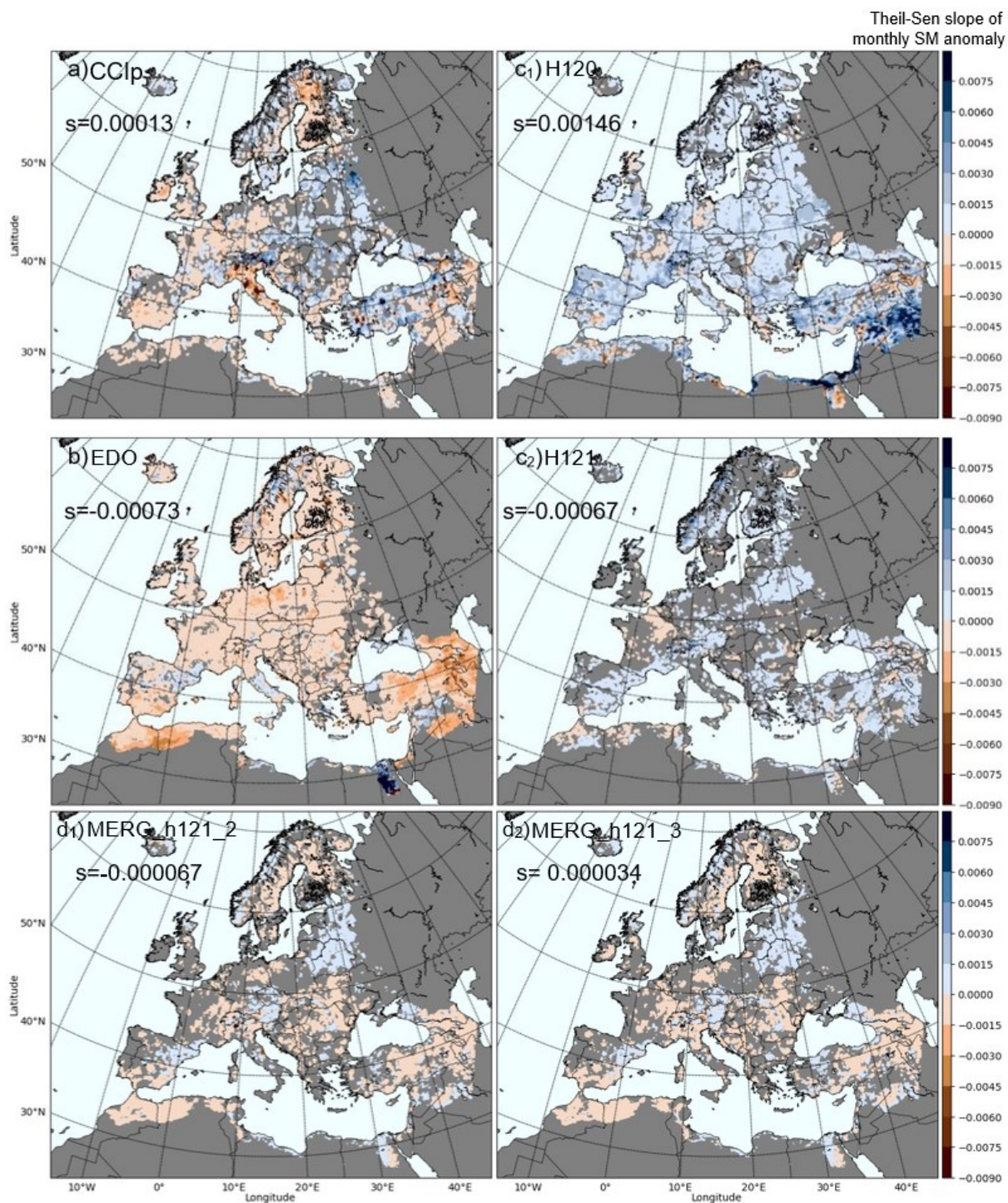
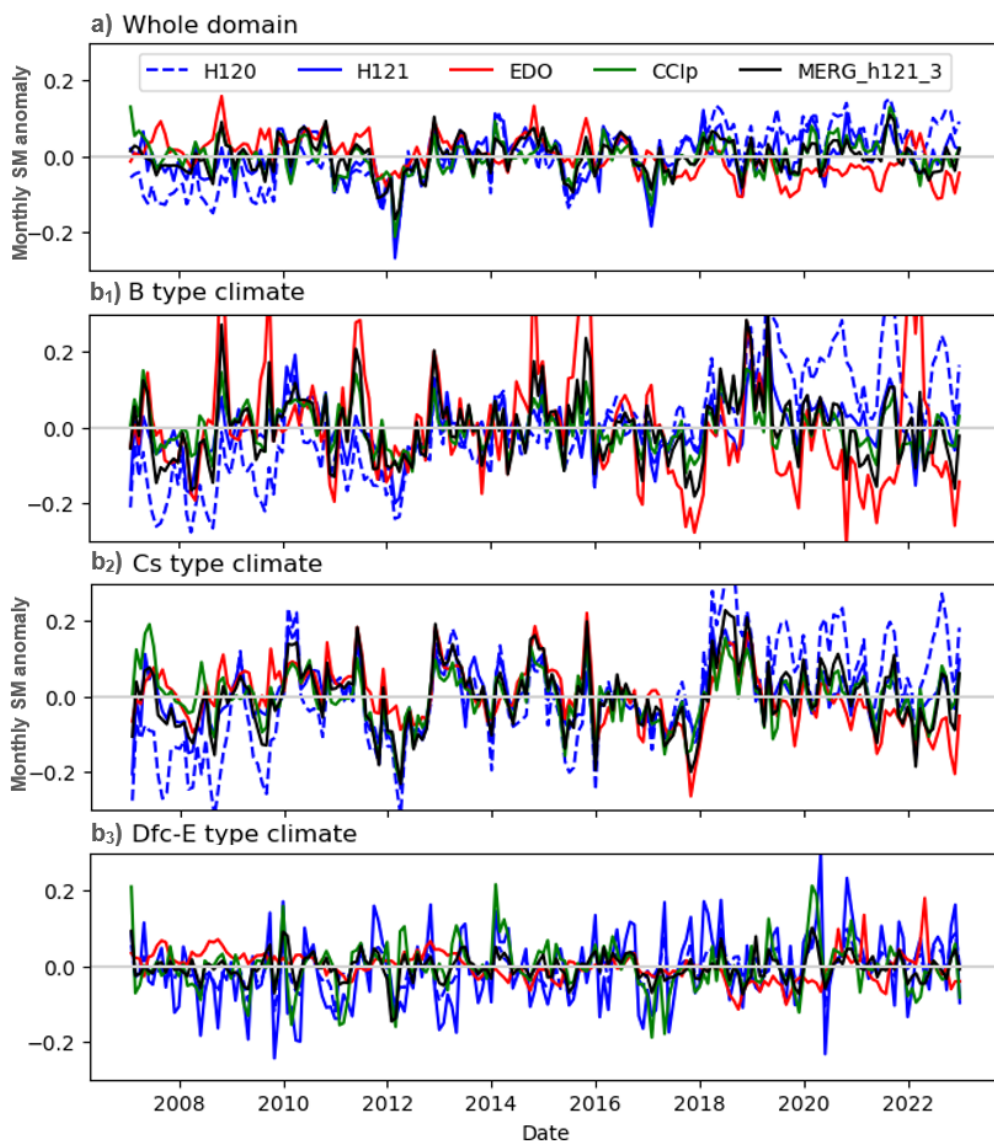


**Figure 9:** Maps of significant annual trends (Theil-Sen slopes) of the series of monthly SM anomalies indicated by the Mann-Kendall tests of a) CCIP, b) EDO, c<sub>1</sub>) H120 and c<sub>2</sub>) H121, and the merged products d<sub>1</sub>) MERG\_h121\_2 and d<sub>2</sub>) MERG\_h121\_3 for the period 2007-2022. Non-significant areas in the plain gray color of the rest of continental areas outside of the domain of study. 'S' describes overall slope values.



435 Interestingly, both merged products (Figs. 9d<sub>1</sub> and d<sub>2</sub>) agree to a great extent, which suggest that the role of CCIP might be already secondary when H121 and EDO become merged. Such agreement in between the two may also imply that the dominance of H121 as best product (Fig. 6) is due to the already consistent nature of H121 or alternatively that H121 and CCIP are both in great agreement. Though, by adopting H121 the significant areas formerly dominating EDO or H120 become no longer the norm, and also reduced compared to CCIP (Fig. 9b vs. d<sub>1</sub> and d<sub>2</sub>). Therefore, merged products compile the trendy areas with more consensus in sign, magnitude and location in between the products, which can be considered as a consistent depiction of the major trends.



440 **Figure 10: Temporal trends of the RS (H120 / H121, CCIP), model-based (EDO) and merged SM products for the whole domain and period of study 2007-2022 of the monthly SM anomalies. (b) Temporal trends of the SM products of EDO (in green continuous**



**line), H120 (in discontinuous blue line) and CCIp (in red line) in the study period 2007-2022, assessed by the main climatic classes of Europe b1) B, b2) Cs, b3) Dfc-E.**

445 The cause of the SM trend shown by EDO (Fig 9b) may seem attributable to global warming origin based on what is widely accepted to be impact of climate change or based on previous reports using reanalysis and model-based studies (Samaniego et al., 2018; Li et al., 2020). The drying trend has been shown to prevail in EDO (Dorigo et al., 2012; Almendra et al., 2022) at least in southern latitudes (Cammalleri et al., 2016). However, many areas of low dry trend in EDO do not concur with the drying areas of H120 / H121 and CCIp (Fig. 9), especially in the SE or NE of the domain where mixed and wetting trends of H120 and CCIp have been described (Tuel and Eltahir, 2021, Saffiotti et al., 2016), but partially agrees reports of SM sensitivity to temperature change using GLDAS (Gu et al., 2019). Therefore, it is still appropriate to contrast SM trends with those of  
450 related variables such as precipitation, evapotranspiration, temperature (Meng et al., 2018; Deng et al., 2019) or even with the response of vegetation (Liu et al., 2020; Lal et al., 2023). The temperature influence may suggest that EDO overexpresses SM trends due to sensitivity to meteorological forcing (Koster et al., 2009). The EDO series over most temperature-driven climates (e.g. B-type, Fig. 10b<sub>1</sub>) partially agree with that.

455 However, the EDO singular trends may imply persisting drifts. This possibility emphasizes the need to carefully revise trends before use. The successful upgrading of the active dataset from H120 to H121 version illustrates the increasing consistency of RS and modelled SM products, whose regular new releases incorporate improvements on processing (subsurface backscattering: Wagner et al., 2022; vegetation: Vreugdenhil et al., 2016) and decreases on their dependence from proxies (Dorigo et al., 2017; Madelon et al., 2021).

460 The sequence of wet and dry spells displayed in the time series of Fig. 10a give the temporal detail of the spatial patterns shown on Fig. 9. The temporal divergence of the trends between EDO and H120 is visible in time series of the whole domain (Fig. 10a) and in the ones of the climate types (Fig. 10b<sub>1</sub>-b<sub>3</sub>), particularly in the last years. Areas of B and Cs climates seem the most affected, followed by Dsb, Dfb, Cfb, Dfa, with Dfc-E as the least affected, in line with the temperature gradient. An  
465 example is the contrast between the former patches of SM increase identified in the period 1988-2010/2015 (Dorigo et al., 2012; Albergel et al., 2013a; Liu et al., 2019), Piles et al., 2019), and the decline reported recently (Skulovich et al., 2023) or in the past (Deng et al., 2019). The best merged product, MERG\_h121\_3 show in Fig. 10 has the advantage of an overly balanced trend. Combining the diverging trends of H120 and EDO may have neutralized the trend in MERG\_h121\_3 and foster its insensitivity to the climate (Fig. 10b<sub>1</sub>-b<sub>6</sub>). A balanced spatial and temporal consistency of the merged product as a  
470 result of combining the diverging trends of the individual products is preferable towards operational monitoring but it may well obscure the interpretation of the causes behind the diverging trends of its components. However, when products with diverging trends counteract, such as between EDO and H120, MERG\_h121\_2 largely agrees with the extension and significance of the trendy areas of CCIp. Thus, merged products can provide better temporal stability than the products used in their combination which is of benefit not only for operational monitoring but for long-term change analysis as well.



## 475 5 Conclusions

The evolution of soil moisture is crucial for identifying alterations of the water cycle and the climate. However, assessing soil moisture change without regarding product-specific uncertainties may cause misleading interpretations. Well-known global soil moisture products such as the remote sensing active H SAF ASCAT-SSM-CDR-12.5km-v7 (H120) and v8 (H121), the passive ESA CCIp and the model-based EDO represent the three main different types of data suitable for soil moisture  
480 monitoring at continental scale, each with specific strengths and weaknesses. This study evaluates their spatial and temporal consistency and their combined potential for operational monitoring of soil moisture.

The correspondence of EDO, CCIp and H120 or H121 shown in pairwise correlation and TCA proved notably consistent in between products for most regions across Europe. The remote sensing datasets H120 and H121 and CCIp can provide equal  
485 or better soil moisture estimates across most of the continent than EDO, prevailing CCIp over temperate oceanic (*C* type of Köppen-Geiger classification) and H120 / H121 over temperate continental climates (*D* type). Conversely EDO, as a model-based type of data is still best at characterizing SM over areas experiencing RS uncertainties due to rough terrain, subsurface scattering or snow prevalence.

490 Compared to in situ data from ISMN networks, products depict a notably reliable characterization of soil moisture, also across climates except for boreal ones (*Dfc-E* type) and despite the uncertainties due to network's particularities. Nonetheless, the passive RS CCIp and the model-based EDO, despite their spatial agreement and adequate comparability to in-situ data, still exhibit residual trends that obscure the interpretation of authentic soil moisture tendencies, either in location, magnitude and significance. CCIp, while of balanced distribution between positive and negative trends over the continent, tends to display  
495 spots of excessive trend over small areas which disagree in sign and magnitude with other products. Conversely, EDO exhibits a tendency to show extensive areas of significant negative trends. The known positive trends of H120 have been corrected in H121 improving the sign magnitude, extent and significance of the trend portrayal. Yet, the overall trend agreement among products remains moderate.

500 Known these uncertainties, the need of refinement of the products but also their complementary advantages and their increasing accuracy, the merging of different types of SM data based on their spatial and temporal scores provides equal or better soil moisture characterization than individual datasets alone, while allowing monitoring across a wider range of conditions. The merging additionally informs about the relative contribution of the distinct types of datasets as well as their added value to near-real time operational monitoring. Consequently, it is encouraged to carefully understand SM products capabilities and to  
505 explore the value of their combination in order to fully exploit their potential for operational soil moisture monitoring.



## 6 Competing interests

The contact author has declared that none of the authors has any competing interests.

## 7 Acknowledgements

The authors acknowledge funding from the European Union “Open Earth Monitor Cyberinfrastructure” project (grant agreement No. 101059548), the EUMETSAT “Satellite Application Facility on Support to Operational Hydrology and Water Management (H SAF) CDOP 4” project (grant no. SAF/H SAF/CDOP4/AGR/01) and the Italian Department of Civil Protection.

## References

- Albergel, C., Rüdiger, C., Pellarin, T., Calvet, J. C., Fritz, N., Froissard, F., ... and Martin, E.: From near-surface to root-zone soil moisture using an exponential filter: an assessment of the method based on in-situ observations and model simulations, *Hydrol. Earth Syst. Sci.*, 12(6), 1323-1337, doi: 10.5194/hess-12-1323-2008, 2008.
- Albergel, C., De Rosnay, P., Gruhier, C., Muñoz-Sabater, J., Hasenauer, S., Isaksen, L., ... and Wagner, W.: Evaluation of remotely sensed and modelled soil moisture products using global ground-based in situ observations, *Remote Sens. Environ.*, 118, 215-226, doi: 10.1016/j.rse.2011.11.017, 2012.
- Albergel, C., Dorigo, W., Reichle, R. H., Balsamo, G., De Rosnay, P., Muñoz-Sabater, J., ... and Wagner, W.: Skill and global trend analysis of soil moisture from reanalyses and microwave remote sensing, *J. Hydrometeorol.*, 14(4), 1259-1277, doi: 10.1175/JHM-D-12-0161.1, 2013a.
- Albergel, C., Dorigo, W., Balsamo, G., Muñoz-Sabater, J., de Rosnay, P., Isaksen, L., ... and Wagner, W.: Monitoring multi-decadal satellite earth observation of soil moisture products through land surface reanalyses, *Remote Sens. Environ.*, 138, 77-89, doi: 10.1016/j.rse.2013.07.009, 2013b.
- Almendra-Martín, L., Martínez-Fernández, J., Piles, M., González-Zamora, Á., Benito-Verdugo, P., and Gaona, J.: Analysis of soil moisture trends in Europe using rank-based and empirical decomposition approaches, *Glob. Planet. Change*, 215, 103868, doi: 10.1016/j.gloplacha.2022.103868, 2022.



- Al-Yaari, A., Wigneron, J. P., Ducharne, A., Kerr, Y. H., Wagner, W., De Lannoy, G., ... and Mialon, A.: Global-scale  
535 comparison of passive (SMOS) and active (ASCAT) satellite-based microwave soil moisture retrievals with soil moisture  
simulations (MERRA-Land), *Remote Sens. Environ.*, 152, 614-626, doi: 10.1016/j.rse.2014.07.013, 2014.
- Al-Yaari, A., Wigneron, J. P., Dorigo, W., Colliander, A., Pellarin, T., Hahn, S., ... and De Lannoy, G.: Assessment and inter-  
540 comparison of recently developed/reprocessed microwave satellite soil moisture products using ISMN ground-based  
measurements, *Remote Sens. Environ.*, 224, 289-303, doi: 10.1016/j.rse.2019.02.008, 2019.
- Beck, H. E., Zimmermann, N. E., McVicar, T. R., Vergopolan, N., Berg, A., and Wood, E. F.: Present and future Köppen-  
Geiger climate classification maps at 1-km resolution, *Sci. Data*, 5(1), 1-12, doi: 10.1038/sdata.2018.214, 2018.
- 545 Beck, H. E., Pan, M., Miralles, D. G., Reichle, R. H., Dorigo, W. A., Hahn, S., ... and Wood, E. F.: Evaluation of 18 satellite-  
and model-based soil moisture products using in situ measurements from 826 sensors, *Hydrol. Earth Syst. Sci.*, 25(1), 17-40,  
doi: 10.5194/hess-25-17-2021, 2021.
- Bolten, J. D., and Crow, W. T.: Improved prediction of quasi-global vegetation conditions using remotely-sensed surface soil  
550 moisture, *Geophys. Res. Lett.*, 39(19), doi: 10.1029/2012GL053470, 2012.
- Brocca, L., Melone, F., Moramarco, T., and Morbidelli, R.: Spatial-temporal variability of soil moisture and its estimation  
across scales, *Water Resour. Res.*, 46(2), doi: 10.1029/2009WR008016, 2010a.
- 555 Brocca, L., Melone, F., Moramarco, T., Wagner, W., and Hasenauer, S.: ASCAT soil wetness index validation through in situ  
and modeled soil moisture data in central Italy, *Remote Sens. Environ.*, 114(11), 2745-2755, doi: 10.1016/j.rse.2010.06.009,  
2010b.
- Brocca, L., Hasenauer, S., Lacava, T., Melone, F., Moramarco, T., Wagner, W., ... and Bittelli, M.: Soil moisture estimation  
560 through ASCAT and AMSR-E sensors: An intercomparison and validation study across Europe, *Remote Sens. Environ.*,  
115(12), 3390-3408, doi: 10.1016/j.rse.2011.08.003, 2011.
- Brocca, L., Ciabatta, L., Moramarco, T., Ponziani, F., Berni, N., and Wagner, W.: Use of satellite soil moisture products for  
the operational mitigation of landslides risk in central Italy, In *Satellite soil moisture retrieval* (pp. 231-247), Elsevier, doi:  
565 10.1016/B978-0-12-803388-3.00012-7, 2016.



- Brocca, L., Ciabatta, L., Massari, C., Camici, S., and Tarpanelli, A.: Soil moisture for hydrological applications: Open questions and new opportunities, *Water*, 9(2), 140, doi: 10.3390/w9020140, 2017.
- 570 Brocca, L., Crow, W. T., Ciabatta, L., Massari, C., De Rosnay, P., Enenkel, M., ... and Wagner, W.: A review of the applications of ASCAT soil moisture products, *IEEE J. Sel. Top. Appl. Earth Obs. Remote. Sens.*, 10(5), 2285-2306, doi: 10.1109/JSTARS.2017.2651140, 2017b.
- Cammalleri, C., Micale, F., and Vogt, J.: On the value of combining different modelled soil moisture products for European  
575 drought monitoring, *J. Hydrol.*, 525, 547-558, doi: 10.1016/j.jhydrol.2015.04.021, 2015.
- Cammalleri, C., Micale, F., and Vogt, J.: Recent temporal trend in modelled soil water deficit over Europe driven by meteorological observations, *Int. J. Climatol.*, 36(15), 4903-4912, doi: 10.1002/joc.4677, 2016.
- 580 Cammalleri, C., Vogt, J. V., Bisselink, B., and de Roo, A. Comparing soil moisture anomalies from multiple independent sources over different regions across the globe, *Hydrol. Earth Syst. Sci.*, 21(12), 6329-6343, doi: 10.5194/hess-21-6329-2017, 2017.
- Chen, F., Crow, W. T., Bindlish, R., Colliander, A., Burgin, M. S., Asanuma, J., and Aida, K.: Global-scale evaluation of  
585 SMAP, SMOS and ASCAT soil moisture products using triple collocation, *Remote Sens. Environ.*, 214, 1-13, doi: 10.1016/j.rse.2018.05.008, 2018.
- Crosson, W. L., Limaye, A. S., and Laymon, C. A.: Parameter sensitivity of soil moisture retrievals from airborne C-and X-band radiometer measurements in SMEX02, *IEEE Trans. Geosci. Remote Sens.*, 43(12), 2842-2853, doi:  
590 10.1109/TGRS.2005.857916, 2005.
- Deng, Y., Wang, S., Bai, X., Luo, G., Wu, L., Cao, Y., ... and Tian, S.: Variation trend of global soil moisture and its cause analysis, *Ecol. Indic.*, 110, 105939, doi: 10.1016/j.ecolind.2019.105939, 2020.
- 595 Denissen, J. M., Teuling, A. J., Reichstein, M., and Orth, R.: Critical soil moisture derived from satellite observations over Europe, *J. Geophys. Res. Atmospheres*, 125(6), e2019JD031672, doi: 10.1029/2019JD031672, 2020.
- De Roo, A. P. J., Wesseling, C. G., and Van Deursen, W. P. A.: Physically based river basin modelling within a GIS: the LISFLOOD model, *Hydrol. Process.*, 14(11-12), 1981-1992, doi: 10.1002/1099-1085(20000815/30)14:11/12<1981::AID-HYP49>3.0.CO;2-F, 2000.  
600



- Dirmeyer, P. A., Gao, X., Zhao, M., Guo, Z., Oki, T., and Hanasaki, N.: GSWP-2: Multimodel analysis and implications for our perception of the land surface, *Bull. Am. Meteorol. Soc.*, 87(10), 1381-1398, doi: 10.1175/BAMS-87-10-1381, 2006.
- 605 Dong, J., and Crow, W. T.: An improved triple collocation analysis algorithm for decomposing autocorrelated and white soil moisture retrieval errors, *Journal of Geophys. Res. Atmospheres*, 122(24), 13-081, doi: 10.1002/2017JD027387, 2017.
- Dorigo, W. A., Scipal, K., Parinussa, R. M., Liu, Y. Y., Wagner, W., De Jeu, R. A., and Naeimi, V.: Error characterisation of global active and passive microwave soil moisture datasets, *Hydrol. Earth Syst. Sci.*, 14(12), 2605-2616, doi: 10.5194/hess-610 14-2605-2010, 2010.
- Dorigo, W. A., Wagner, W., Hohensinn, R., Hahn, S., Paulik, C., Xaver, A., Gruber, A., Drusch, M., Mecklenburg, S., van Oevelen, P., Robock, A., and Jackson, T.: The International Soil Moisture Network: a data hosting facility for global in situ soil moisture measurements, *Hydrol. Earth Syst. Sci.*, 15, 1675-1698, doi: 10.5194/hess-15-1675-2011, 2011.
- 615 Dorigo, W., De Jeu, R., Chung, D., Parinussa, R., Liu, Y., Wagner, W., and Fernández-Prieto, D.: Evaluating global trends (1988–2010) in harmonized multi-satellite surface soil moisture, *Geophys. Res. Lett.*, 39(18), doi: 10.1029/2012GL052988, 2012.
- 620 Dorigo, W. A., Gruber, A., De Jeu, R. A. M., Wagner, W., Stacke, T., Loew, A., ... and Kidd, R.: Evaluation of the ESA CCI soil moisture product using ground-based observations, *Remote Sens. Environ.*, 162, 380-395, doi: 10.1016/j.rse.2014.07.023, 2015.
- Dorigo, W., Wagner, W., Albergel, C., Albrecht, F., Balsamo, G., Brocca, L., ... and Lecomte, P.: ESA CCI Soil Moisture for improved Earth system understanding: State-of-the art and future directions, *Remote Sens. Environ.*, 203, 185-215, doi: 10.1016/j.rse.2017.07.001, 2017.
- 625 Dorigo, W., Himmelbauer, I., Aberer, D., Schremmer, L., Petrakovic, I., Zappa, L., ... and Sabia, R.: The International Soil Moisture Network: serving Earth system science for over a decade, *Hydrol. Earth Syst. Sci.*, 25(11), 5749-5804, doi: 630 10.5194/hess-25-5749-2021, 2021.
- Draper, C. S., Walker, J. P., Steinle, P. J., De Jeu, R. A., and Holmes, T. R.: An evaluation of AMSR–E derived soil moisture over Australia, *Remote Sens. Environ.*, 113(4), 703-710, doi: 10.1016/j.rse.2008.11.011, 2009.



- 635 Duygu, M. B., and Akyürek, Z.: Using cosmic-ray neutron probes in validating satellite soil moisture products and land surface models, *Water*, 11(7), 1362, doi: 10.3390/w11071362, 2019.
- Entekhabi, D., Njoku, E. G., O'Neill, P. E., Kellogg, K. H., Crow, W. T., Edelstein, W. N., ... and Van Zyl, J.: The soil moisture active passive (SMAP) mission, *Proc. IEEE*, 98(5), 704-716, doi: 10.1109/JPROC.2010.2043918, 2010.
- 640 Escorihuela, M. J., and Quintana-Seguí, P.: Comparison of remote sensing and simulated soil moisture datasets in Mediterranean landscapes, *Remote Sens. Environ.*, 180, 99-114, doi: 10.1016/j.rse.2016.02.046, 2016.
- Fan, X., Lu, Y., Liu, Y., Li, T., Xun, S., and Zhao, X.: Validation of multiple soil moisture products over an intensive  
645 agricultural region: Overall accuracy and diverse responses to precipitation and irrigation events, *Remote Sens.*, 14(14), 3339, doi: 10.3390/rs14143339, 2022.
- Fatichi, S., Vivoni, E. R., Ogden, F. L., Ivanov, V. Y., Mirus, B., Gochis, D., ... and Tarboton, D.: An overview of current applications, challenges, and future trends in distributed process-based models in hydrology, *J. Hydrol.*, 537, 45-60, doi:  
650 10.1016/j.jhydrol.2016.03.026, 2016.
- Feng, H., and Zhang, M.: Global land moisture trends: drier in dry and wetter in wet over land, *Sci. Rep.*, 5(1), 18018, doi: 10.1038/srep18018, 2015.
- 655 Filippucci, P., Brocca, L., Massari, C., Saltalippi, C., Wagner, W., and Tarpanelli, A.: Toward a self-calibrated and independent SM2RAIN rainfall product, *J. Hydrol.*, 603, 126837, doi: 10.1016/j.jhydrol.2021.126837, 2021.
- Ford, T. W., McRoberts, D. B., Quiring, S. M., and Hall, R. E.: On the utility of in situ soil moisture observations for flash drought early warning in Oklahoma, USA, *Geophys. Res. Lett.*, 42(22), 9790-9798, doi: 10.1002/2015GL066600, 2015.
- 660 Gimeno, L., Stohl, A., Trigo, R. M., Dominguez, F., Yoshimura, K., Yu, L., ... and Nieto, R.: Oceanic and terrestrial sources of continental precipitation, *Rev. Geophys.*, 50(4), doi: 10.1029/2012RG000389, 2012.
- Green, J. K., Seneviratne, S. I., Berg, A. M., Findell, K. L., Hagemann, S., Lawrence, D. M., and Gentine, P.: Large influence  
665 of soil moisture on long-term terrestrial carbon uptake, *Nature*, 565(7740), 476-479, doi: 10.1038/s41586-018-0848-x, 2019.



- 670 Gruber, A., Dorigo, W. A., Zwieback, S., Xaver, A., and Wagner, W.: Characterizing coarse-scale representativeness of in situ soil moisture measurements from the International Soil Moisture Network, *Vadose Zone J.*, 12(2), 1-16, doi: 10.2136/vzj2012.0170, 2013.
- Gruber, A., Su, C. H., Zwieback, S., Crow, W., Dorigo, W., and Wagner, W.: Recent advances in (soil moisture) triple collocation analysis, *Int. J. Appl. Earth Obs. Geoinf.*, 45, 200-211, doi: 10.1016/j.jag.2015.09.002, 2016.
- 675 Gruber, A., Dorigo, W. A., Crow, W., and Wagner, W.: Triple collocation-based merging of satellite soil moisture retrievals, *IEEE Trans. Geosci. Remote Sens.*, 55(12), 6780-6792, doi: 10.1109/TGRS.2017.2734070, 2017.
- Gruber, A., Scanlon, T., van der Schalie, R., Wagner, W., and Dorigo, W.: Evolution of the ESA CCI Soil Moisture climate data records and their underlying merging methodology, *Earth Syst. Sci. Data*, 11(2), 717-739, doi: 10.5194/essd-11-717-2019, 2019.
- 680 Gruber, A., De Lannoy, G., Albergel, C., Al-Yaari, A., Brocca, L., Calvet, J. C., ... and Wagner, W.: Validation practices for satellite soil moisture retrievals: What are (the) errors?, *Remote Sens. Environ.*, 244, 111806, doi: 10.1016/j.jag.2015.10.007, 2020.
- 685 Gu, X., Zhang, Q., Li, J., Singh, V. P., Liu, J., Sun, P., ... and Wu, J.: Intensification and expansion of soil moisture drying in warm season over Eurasia under global warming, *J. Geophys. Res. Atmospheres*, 124(7), 3765-3782, doi: 10.1029/2018JD029776, 2019.
- Hahn, S., Reimer, C., Vreugdenhil, M., Melzer, T., & Wagner, W.: Dynamic characterization of the incidence angle dependence of backscatter using metop ASCAT, *IEEE J. Sel. Top. Appl. Earth Obs. Remote. Sens.*, 10(5), 2348-2359, doi: 690 10.1109/JSTARS.2016.2628523, 2017.
- Ikonen, J., Smolander, T., Rautiainen, K., Cohen, J., Lemmetyinen, J., Salminen, M., and Pulliainen, J.: Spatially distributed evaluation of ESA CCI Soil Moisture products in a northern boreal forest environment, *Geosci.*, 8(2), 51, doi: 695 10.3390/geosciences8020051, 2018.
- Juglea, S., Kerr, Y., Mialon, A., Wigneron, J. P., Lopez-Baeza, E., Cano, A., ... and Delwart, S.: Modelling soil moisture at SMOS scale by use of a SVAT model over the Valencia Anchor Station, *Hydrol. Earth Syst. Sci.*, 14(5), 831-846, doi: 10.5194/hess-14-831-2010, 2010.

700



- Harper, K. L., Lamarche, C., Hartley, A., Peylin, P., Ottlé, C., Bastrikov, V., ... and Defourny, P. (2023). A 29-year time series of annual 300 m resolution plant-functional-type maps for climate models, *Earth Syst. Sci. Data*, 15(3), 1465-1499, doi:10.5194/essd-15-1465-2023, 2023.
- 705 Karthikeyan, L., Pan, M., Wanders, N., Kumar, D. N., and Wood, E. F.: 2017. Four decades of microwave satellite soil moisture observations: Part 1. A review of retrieval algorithms, *Adv. Water Resour.*, 109, 106-120, doi: 10.1016/j.advwatres.2017.09.006, 2017.
- Kendall, M. G.: Rank correlation methods, 1948.
- 710
- Kerr, Y. H., Waldteufel, P., Richaume, P., Wigneron, J. P., Ferrazzoli, P., Mahmoodi, A., ... and Delwart, S.: The SMOS soil moisture retrieval algorithm, *IEEE Trans. Geosci. Remote Sens.*, 50(5), 1384-1403, doi: 10.1109/TGRS.2012.2184548, 2012.
- Kim, S. B., Moghaddam, M., Tsang, L., Burgin, M., Xu, X., and Njoku, E. G.: Models of L-band radar backscattering coefficients over global terrain for soil moisture retrieval, *IEEE Trans. Geosci. Remote Sens.*, 52(2), 1381-1396, doi: 10.1109/TGRS.2013.2250980, 2013.
- 715
- Kim, H., Wigneron, J. P., Kumar, S., Dong, J., Wagner, W., Cosh, M. H., ... and Lakshmi, V.: Global scale error assessments of soil moisture estimates from microwave-based active and passive satellites and land surface models over forest and mixed irrigated/dryland agriculture regions, *Remote Sens. Environ.*, 251, 112052, doi: 10.1016/j.rse.2020.112052, 2020.
- 720
- Kolassa, J., Gentine, P., Prigent, C., Aires, F., and Alemohammad, S. H.: Soil moisture retrieval from AMSR-E and ASCAT microwave observation synergy. Part 2: Product evaluation, *Remote Sens. Environ.*, 195, 202-217, doi: 10.1016/j.rse.2017.04.020, 2017.
- 725
- Koster, R. D., Guo, Z., Yang, R., Dirmeyer, P. A., Mitchell, K., and Puma, M. J.: On the nature of soil moisture in land surface models, *J. Clim.*, 22(16), 4322-4335, 2009.
- Künzer, C., Bartalis, Z., Schmidt, M., Zhao, D., and Wagner, W.: Trend analyses of a global soil moisture time series derived from ERS-1/-2 scatterometer data: floods, droughts and long term changes, *Int. Arch. Photogramm., Remote Sens. Spat. Inf. Sci.*, 37, 1363-1368, 2008.
- 730
- Lal, P., Shekhar, A., Gharun, M., and Das, N. N.: Spatiotemporal evolution of global long-term patterns of soil moisture, *Sci. Total Environ.*, 867, 161470, doi: 10.1016/j.scitotenv.2023.161470, 2023.



735

Laguardia, G., and Niemeyer, S.: On the comparison between the LISFLOOD modelled and the ERS/SCAT derived soil moisture estimates, *Hydrol. Earth Syst. Sci.*, 12(6), 1339-1351, doi: 10.5194/hess-12-1339-2008, 2008.

740

Leroux, D. J., Kerr, Y. H., Richaume, P., and Fieuzal, R.: Spatial distribution and possible sources of SMOS errors at the global scale, *Remote Sens. Environ.*, 133, 240-250, doi: 10.1016/j.rse.2013.02.017, 2013.

Li, M., Wu, P., and Ma, Z.: A comprehensive evaluation of soil moisture and soil temperature from third-generation atmospheric and land reanalysis data sets, *Int. J. Climatol.*, 40(13), 5744-5766, doi: 10.1002/joc.6549, 2020.

745

Li, Y., van Dijk, A. I., Tian, S., and Renzullo, L. J.: Skill and lead time of vegetation drought impact forecasts based on soil moisture observations, *J. Hydrol.*, 620, 129420, doi: 10.1016/j.jhydrol.2023.129420, 2023.

Liu, L., Gudmundsson, L., Hauser, M., Qin, D., Li, S., and Seneviratne, S. I.: Soil moisture dominates dryness stress on ecosystem production globally, *Nat. Commun.*, 11(1), 4892, doi: 10.1038/s41467-020-18631-1, 2020.

750

Liu, Y. Y., Dorigo, W. A., Parinussa, R. M., de Jeu, R. A., Wagner, W., McCabe, M. F., ... and Van Dijk, A. I. J. M.: Trend-preserving blending of passive and active microwave soil moisture retrievals, *Remote Sens. Environ.*, 123, 280-297, doi: 10.1016/j.rse.2012.03.014, 2012.

755

Liu, Y., Liu, Y., and Wang, W.: Inter-comparison of satellite-retrieved and Global Land Data Assimilation System-simulated soil moisture datasets for global drought analysis, *Remote Sens. Environ.*, 220, 1-18. doi: 10.1016/j.rse.2018.10.026, 2019.

760

Loew, A., Stacke, T., Dorigo, W., De Jeu, R., and Hagemann, S.: Potential and limitations of multidecadal satellite soil moisture observations for selected climate model evaluation studies, *Hydrol. Earth Syst. Sci.*, 17(9), 3523-3542, doi: 10.5194/hess-17-3523-2013, 2013.

765

Lun, D., Viglione, A., Bertola, M., Komma, J., Parajka, J., Valent, P., and Blöschl, G.: Characteristics and process controls of statistical flood moments in Europe—a data-based analysis, *Hydrol. Earth Syst. Sci.*, 25(10), 5535-5560, doi: <https://doi.org/10.5194/hess-25-5535-2021>, 2021.

Ma, H., Zeng, J., Chen, N., Zhang, X., Cosh, M. H., and Wang, W.: Satellite surface soil moisture from SMAP, SMOS, AMSR2 and ESA CCI: A comprehensive assessment using global ground-based observations, *Remote Sens. Environ.*, 231, 111215, doi: 10.1016/j.rse.2019.111215, 2019.



- 770 Madelon, R., Rodríguez-Fernández, N. J., van der Schalie, R., Scanlon, T., Al Bitar, A., Kerr, Y. H., ... and Dorigo, W.:  
Toward the Removal of Model Dependency in Soil Moisture Climate Data Records by Using an L-Band Scaling Reference,  
IEEE J. Sel. Top. Appl. Earth Obs. Remote Sens., 15, 831-848, doi: 10.1109/JSTARS.2021.3137008, 2021.
- Mann, H. B.: Nonparametric tests against trend, *Econometrica: J. Econom.*, 245-259, 1945.
- 775 Markonis, Y., and Strnad, F.: Representation of European hydroclimatic patterns with self-organizing maps, *Holocene*, 30(8),  
1155-1162, doi: 10.1177/0959683620913924, 2020.
- Massari, C., Crow, W. and Brocca, L.: An assessment of the performance of global rainfall estimates without ground-based  
780 observations, *Hydrol. Earth Syst. Sci.*, 21.9 (2017): 4347-4361, doi: 10.5194/hess-21-4347-2017, 2017.
- Mazzariello, A., Albano, R., Lacava, T., Manfreda, S., and Sole, A.: Intercomparison of recent microwave satellite soil  
moisture products on European ecoregions, *J. Hydrol.*, 626, 130311, doi: 10.1016/j.jhydrol.2023.130311, 2023.
- 785 McColl, K. A., Vogelzang, J., Konings, A. G., Entekhabi, D., Piles, M., and Stoffelen, A.: Extended triple collocation:  
Estimating errors and correlation coefficients with respect to an unknown target, *Geophys. Res. Lett.*, 41(17), 6229-6236, doi:  
10.1002/2014GL061322, 2014.
- McColl, K. A., Entekhabi, D., and Piles, M.: Uncertainty analysis of soil moisture and vegetation indices using Aquarius  
790 scatterometer observations, *IEEE Trans. Geosci. Remote Sens.*, 52(7), 4259-4272, doi: 10.1109/TGRS.2013.2280701, 2013.
- Meng, X., Li, R., Luan, L., Lyu, S., Zhang, T., Ao, Y., ... and Ma, Y.: Detecting hydrological consistency between soil moisture  
and precipitation and changes of soil moisture in summer over the Tibetan Plateau, *Clim. Dyn.*, 51, 4157-4168, doi:  
10.1007/s00382-017-3646-5, 2018.
- 795 Mohammed, P. N., Aksoy, M., Piepmeier, J. R., Johnson, J. T., and Bringer, A.: SMAP L-band microwave radiometer: RFI  
mitigation prelaunch analysis and first year on-orbit observations, *IEEE Trans. Geosci. Remote. Sens.*, 54(10), 6035-6047, doi:  
10.1109/TGRS.2016.2580459, 2016.
- 800 Naeimi, V., Scipal, K., Bartalis, Z., Hasenauer, S., and Wagner, W.: An improved soil moisture retrieval algorithm for ERS  
and METOP scatterometer observations, *IEEE Trans. Geosci. Remote. Sens.*, 47(7), 1999-2013, doi:  
10.1109/TGRS.2008.2011617, 2009.



805 Naeimi, V., Paulik, C., Bartsch, A., Wagner, W., Kidd, R., Park, S. E., ... and Boike, J.: ASCAT Surface State Flag (SSF):  
Extracting information on surface freeze/thaw conditions from backscatter data using an empirical threshold-analysis  
algorithm, *IEEE Trans. Geosci. Remote Sens.*, 50(7), 2566-2582, doi: 10.1109/TGRS.2011.2177667, 2012.

810 Njoku, E. G., Jackson, T. J., Lakshmi, V., Chan, T. K., and Nghiem, S. V.: Soil moisture retrieval from AMSR-E, *IEEE Trans.  
Geosci. Remote Sens.*, 41(2), 215-229, doi: 10.1109/TGRS.2002.808243, 2003.

Ochsner, T. E., Cosh, M. H., Cuenca, R. H., Dorigo, W. A., Draper, C. S., Hagimoto, Y., ... and Zreda, M.: State of the art in  
large-scale soil moisture monitoring, *Soil Sci. Soc. Am. J.*, 77(6), 1888-1919, doi: 10.2136/sssaj2013.03.0093, 2013.

815 Oliva, R., Daganzo, E., Richaume, P., Kerr, Y., Cabot, F., Soldo, Y., ... and Lopes, G.: Status of Radio Frequency Interference  
(RFI) in the 1400–1427 MHz passive band based on six years of SMOS mission, *Remote Sens. Environ.*, 180, 64-75, doi:  
10.1016/j.rse.2016.01.013, 2016.

820 Owe, M., Van de Griend, A. A., De Jeu, R., De Vries, J. J., Seyhan, E., and Engman, E. T.: Estimating soil moisture from  
satellite microwave observations: Past and ongoing projects, and relevance to GCIP, *J. Geophys. Res.*, 104(D16), 19735-  
19742, doi: 10.1029/1999JD900107, 1999.

825 Parinussa, R. M., Yilmaz, M. T., Anderson, M. C., Hain, C. R., and De Jeu, R. A. M.: An intercomparison of remotely sensed  
soil moisture products at various spatial scales over the Iberian Peninsula, *Hydrol. Process.*, 28(18), 4865-4876, doi:  
10.1002/hyp.9975, 2014.

Paulik, C., Dorigo, W., Wagner, W., and Kidd, R.: Validation of the ASCAT Soil Water Index using in situ data from the  
International Soil Moisture Network, *Int. J. Appl. Earth Obs. Geoinformation*, 30, 1-8, doi: 10.1016/j.jag.2014.01.007, 2014.

830 Pellarin, T., Calvet, J. C., & Wagner, W.: Evaluation of ERS scatterometer soil moisture products over a half-degree region in  
southwestern France, *Geophys. Res. Lett.*, 33(17), doi: 10.1029/2006GL027231, 2006.

Peng, J., Loew, A., Merlin, O., & Verhoest, N. E.: A review of spatial downscaling of satellite remotely sensed soil moisture,  
*Rev. Geophys.*, 55(2), 341-366, doi: 10.1002/2016RG000543, 2017.



- 835 Peng, J., Albergel, C., Balenzano, A., Brocca, L., Cartus, O., Cosh, M. H., ... and Loew, A.: A roadmap for high-resolution satellite soil moisture applications—confronting product characteristics with user requirements, *Remote Sens. Environ.*, 252, 112162, doi: 10.1016/j.rse.2020.112162, 2021a.
- Peng, J., Tanguy, M., Robinson, E. L., Pinnington, E., Evans, J., Ellis, R., ... and Dadson, S.: Estimation and evaluation of  
840 high-resolution soil moisture from merged model and Earth observation data in the Great Britain, *Remote Sens. Environ.*, 264, 112610, doi: 10.1016/j.rse.2021.112610, 2021b.
- Petropoulos, G. P., Ireland, G., & Barrett, B.: Surface soil moisture retrievals from remote sensing: Current status, products & future trends, *Phys. Chem. Earth, Parts A/B/C*, 83, 36-56, doi: 10.1016/j.pce.2015.02.009, 2015.
- 845 Pfeil, I., Vreugdenhil, M., Hahn, S., Wagner, W., Strauss, P., and Blöschl, G.: Improving the seasonal representation of ASCAT soil moisture and vegetation dynamics in a temperate climate, *Remote Sens.*, 10(11), 1788, doi:10.3390/rs10111788, 2018.
- Pierdicca, N., Fascetti, F., Pulvirenti, L., Crapolicchio, R., and Muñoz-Sabater, J.: Quadruple collocation analysis for soil  
850 moisture product assessment, *IEEE Geosci. Remote Sens. Lett.*, 12(8), 1595-1599, doi: 10.1109/LGRS.2015.2414654, 2015a.
- Pierdicca, N., Fascetti, F., Pulvirenti, L., Crapolicchio, R., and Muñoz-Sabater, J.: Analysis of ASCAT, SMOS, in-situ and land model soil moisture as a regionalized variable over Europe and North Africa, *Remote Sens. Environ.*, 170, 280-289, doi: 10.1016/j.rse.2015.09.005, 2015b.
- 855 Piles, M., Ballabrera-Poy, J., & Muñoz-Sabater, J.: Dominant features of global surface soil moisture variability observed by the SMOS satellite, *Remote Sens.*, 11(1), 95, doi: 10.3390/rs11010095, 2019.
- Portal, G., Jagdhuber, T., Vall-llossera, M., Camps, A., Pablos, M., Entekhabi, D., and Piles, M.: Assessment of multi-scale  
860 SMOS and SMAP soil moisture products across the Iberian Peninsula, *Remote Sens.* 12(3), 570, doi: 10.3390/rs12030570, 2020.
- Preimesberger, W., Scanlon, T., Su, C. H., Gruber, A., and Dorigo, W.: Homogenization of structural breaks in the global ESA CCI soil moisture multisatellite climate data record, *IEEE Trans. Geosci. Remote Sens.*, 59(4), 2845-2862, doi: 10.1109/TGRS.2020.3012896, 2020.
- 865 Rahmani, A., Golian, S., and Brocca, L.: Multiyear monitoring of soil moisture over Iran through satellite and reanalysis soil moisture products, *Int. J. Appl. Earth Obs. Geoinf.*, 48, 85-95, doi: 10.1016/j.jag.2015.06.009, 2016.



870 Reichle, R. H., and Koster, R. D.: Bias reduction in short records of satellite soil moisture, *Geophys. Res. Lett.*, 31(19), doi:  
10.1029/2004GL020938, 2004.

Rodell, M., Houser, P. R., Jambor, U. E. A., Gottschalck, J., Mitchell, K., Meng, C. J., ... and Toll, D.: The global land data  
assimilation system, *Bull. Am. Meteorol. Soc.*, 85(3), 381-394, doi: 10.1175/BAMS-85-3-381, 2004.

875

Saffioti, C., Fischer, E. M., Scherrer, S. C., and Knutti, R.: Reconciling observed and modeled temperature and precipitation  
trends over Europe by adjusting for circulation variability, *Geophys. Res. Lett.*, 43(15), 8189-8198, doi:  
10.1002/2016GL069802, 2016.

880 Salamon, P., Arnal, L., Asp, S., Baugh, C., Beck, H., Bisselink, B., De Roo, A., Disperati, J., Dottori, F., Garcia-Padilla, M.,  
Garcia-Sanchez, R., Gelati, E., Gomes, G., Kalas, M., Krzeminski, B., Latini, M., Lorini, V., Mazzetti, C., Mikulichova, M.,  
Muraro, D., Prudhomme, C., Rauthe-Schöch, A., Rehfeldt, K., Schweim, C., Skoien, J., Smith, P., Sprokkereef, E., Thiemig,  
V., Wetterhall, F. and Ziese, M., EFAS upgrade for the extended model domain, EUR 29323 EN, Publications Office of the  
European Union, Luxembourg, 2019, ISBN 978-92-79-92881-9, doi:10.2760/806324, JRC111610.

885

Samaniego, L., Kumar, R., and Zink, M.: Implications of parameter uncertainty on soil moisture drought analysis in Germany,  
*J. Hydrometeorol.*, 14(1), 47-68, doi: 10.1175/JHM-D-12-075.1, 2013.

890 Samaniego, L., Thober, S., Kumar, R., Wanders, N., Rakovec, O., Pan, M., ... and Marx, A.: Anthropogenic warming  
exacerbates European soil moisture droughts, *Nat. Clim. Change*, 8(5), 421-426, doi: 10.1038/s41558-018-0138-5, 2018.

Schmugge, T. J.: Remote sensing of soil moisture: Recent advances, *IEEE Trans. Geosci. Remote Sens.*, (3), 336-344, doi:  
10.1109/TGRS.1983.350563, 1983.

895 Scipal, K., Holmes, T., De Jeu, R., Naeimi, V., and Wagner, W.: A possible solution for the problem of estimating the error  
structure of global soil moisture data sets, *Geophys. Res. Lett.*, 35(24), doi: 10.1029/2008GL035599, 2008.

900 Seneviratne, S. I., Corti, T., Davin, E. L., Hirschi, M., Jaeger, E. B., Lehner, I., ... and Teuling, A. J.: Investigating soil  
moisture-climate interactions in a changing climate: A review, *Earth-Sci. Rev.*, 99(3-4), 125-161, doi:  
10.1016/j.earscirev.2010.02.004, 2010.



- Sheffield, J., and Wood, E. F.: Characteristics of global and regional drought, 1950–2000: Analysis of soil moisture data from off-line simulation of the terrestrial hydrologic cycle, *J. Geophys. Res. Atmospheres*, 112(D17), doi: 10.1029/2006JD008288, 2007.
- 905
- Skulovich, O., and Gentine, P.: A Long-term Consistent Artificial Intelligence and Remote Sensing-based Soil Moisture Dataset, *Sci. Data*, 10(1), 154, doi: 10.1038/s41597-023-02053-x, 2023.
- Stoffelen, A.: Toward the true near-surface wind speed: Error modeling and calibration using triple collocation. *J. Geophys. Res. Oceans*, 103(C4), 7755-7766, doi: 10.1029/97JC03180, 1998.
- 910
- Tuel, A., and Eltahir, E. A.: Mechanisms of European summer drying under climate change, *J. Clim.*, 34(22), 8913-8931, doi: 10.1175/JCLI-D-20-0968.1, 2021.
- 915
- Van Der Knijff, J. M., Younis, J., and De Roo, A. P. J.: LISFLOOD: a GIS-based distributed model for river basin scale water balance and flood simulation, *Int. J. Geogr. Inf. Sci.*, 24(2), 189-212, doi: 10.1080/13658810802549154, 2010.
- van der Molen, M. K., De Jeu, R. A. M., Wagner, W., Van Der Velde, I. R., Kolari, P., Kurbatova, J., ... and Peters, W.: The effect of assimilating satellite-derived soil moisture data in SiBCASA on simulated carbon fluxes in Boreal Eurasia, *Hydrol. Earth Syst. Sci.*, 20(2), 605-624, doi: 10.5194/hess-20-605-2016, 2016.
- 920
- Vereecken, H., Schnepf, A., Hopmans, J. W., Javaux, M., Or, D., Roose, T., ... and Young, I. M.: Modeling soil processes: Review, key challenges, and new perspectives, *Vadose Zone J.*, 15(5), doi: 10.2136/vzj2015.09.0131, 2016.
- 925
- Vreugdenhil, M., Dorigo, W. A., Wagner, W., De Jeu, R. A., Hahn, S., and Van Marle, M. J.: Analyzing the vegetation parameterization in the TU-Wien ASCAT soil moisture retrieval, *IEEE Trans. Geosci. Remote Sens.*, 54(6), 3513-3531, doi: 10.1109/TGRS.2016.2519842, 2016.
- Wagner, W., Lemoine, G., and Rott, H.: A method for estimating soil moisture from ERS scatterometer and soil data, *Remote Sens. Environ.*, 70(2), 191-207, doi: 10.1016/S0034-4257(99)00036-X, 1999.
- 930
- Wagner, W., Lindorfer, R., Melzer, T., Hahn, S., Bauer-Marschallinger, B., Morrison, K., ... and Vreugdenhil, M.: Widespread occurrence of anomalous C-band backscatter signals in arid environments caused by subsurface scattering, *Remote Sens. Environ.*, 276, 113025, doi: 10.1016/j.rse.2022.113025, 2022.
- 935



- Wanders, N., Bierkens, M. F., de Jong, S. M., de Roo, A., and Karssenber, D.: The benefits of using remotely sensed soil moisture in parameter identification of large-scale hydrological models, *Water Resour. Res.*, 50(8), 6874-6891, doi: 10.1002/2013WR014639, 2014.
- 940 Wang, Y., Leng, P., Peng, J., Marzahn, P., and Ludwig, R.: Global assessments of two blended microwave soil moisture products CCI and SMOPS with in-situ measurements and reanalysis data, *Int. J. Appl. Earth Obs. Geoinformation*, 94, 102234, doi: 10.1016/j.jag.2020.102234, 2021.
- Wigneron, J. P., Waldteufel, P., Chanzy, A., Calvet, J. C., and Kerr, Y.: Two-dimensional microwave interferometer retrieval capabilities over land surfaces (SMOS mission), *Remote Sens. Environ.*, 73(3), 270-282, doi: 10.1016/S0034-4257(00)00103-6, 2000.
- 945 Wilson, D. J., Western, A. W., and Grayson, R. B.: Identifying and quantifying sources of variability in temporal and spatial soil moisture observations, *Water Resour. Res.*, 40(2), doi: 10.1029/2003WR002306, 2004.
- 950 Yue, S., Pilon, P., & Cavadias, G.: Power of the Mann–Kendall and Spearman's rho tests for detecting monotonic trends in hydrological series, *J. Hydrol.*, 259(1-4), 254-271, doi: 10.1016/S0022-1694(01)00594-7, 2002.
- Zappa, L., Woods, M., Hemment, D., Xaver, A., and Dorigo, W.: Evaluation of remotely sensed soil moisture products using crowdsourced measurements, In Eighth international conference on remote sensing and geoinformation of the environment (RSCy2020) (Vol. 11524, pp. 660-672), SPIE, doi: 10.1117/12.2571913, 2020.
- 955 Zucco, G., Brocca, L., Moramarco, T., and Morbidelli, R.: Influence of land use on soil moisture spatial–temporal variability and monitoring, *J. Hydrol.*, 516, 193-199, doi: 10.1016/j.jhydrol.2014.01.043, 2014.
- 960 Zwieback, S., Hensley, S., and Hajnsek, I.: Soil moisture estimation using differential radar interferometry: Toward separating soil moisture and displacements, *IEEE Trans. Geosci. Remote Sens.*, 55(9), 5069-5083, doi: 10.1109/TGRS.2017.2702099, 2017.